played significantly higher fluorescence intensity than IMFD-70/Ste2p even before inactivation of signaling in IMFD-70/Ste2p (before 12 h). These results indicate that feedback signal activation was successfully invoked even when using an episomal plasmid expression system.

Concentration–response curves of these cells were constructed at 18 h of cultivation (Fig. 3B). Whereas the fluorescence intensity of IMFD-70/Ste2p started to increase from a concentration of approximately 50 nM α-factor and reached a maximum level at 500 nM α-factor, that of IMFD-70B/Ste2p gradually increased between concentrations of 500 pM and 500 nM α-factor. The EC_{50} values were 180 nM (IMFD-70/Ste2p) and 20 nM (IMFD-70B/Ste2p), respectively. A similar tendency in the difference of the dose responses was observed when comparing these strains at each optimal cultivation time (IMFD-70/Ste2p at 12 h and IMFD-70B/Ste2p at 18 h) (see Supplementary Fig. S2A). Increases in GFP fluorescence of the intensity observed in IMFD-70B/Ste2p have never been observed in non-feedback activation systems even at much higher concentrations of α-factor (data not shown). The concentration ranges of agonistic ligand required for signal activation in the episomal plasmid system were much lower than those required in the chromosomal system because of the hypersensitivity caused by the *SST2* deletion. In addition, both the detection limit and the maximum intensity of GFP fluorescence were apparently improved by feedback signal activation in the episomal system.

Feedback signal activation significantly improves the sensitivity of agonist detection, and the response to agonist stimulation, of the hSSTR5 receptor

Somatostatin (SST) is a cyclic neuropeptide known as a growth hormone release-inhibiting factor, and its receptors are therapeutic targets of acromegaly, Cushing's disease, and Alzheimer's disease [26–28]. To investigate whether feedback signal activation successfully rescues the partial activation of human GPCRs (which varies in strength depending on the coupling efficiency of the GPCR with yeast G-proteins) in yeast cells, we assayed SST stimulation of its GPCR, hSSTR5 [11].

An hSSTR5 expression plasmid (pHM-SSTR5) was introduced into IMFD-70 and IMFD-70B strains (Table 1). Each transformant was cultivated in SDM71 medium for signaling assay. Concentration–response curves of these cells were constructed by quantitative evaluation of the GFP fluorescence of both strains after 18 h of cultivation in the presence of several concentrations of SST (Fig. 4A). IMFD-70/hSSTR5 (the common activation strain) displayed a gradual increase in fluorescence intensity at concentrations of SST between 10 nM and 1 μM, and these responses were remarkably similar to those of a previous study [11]. However, the GFP fluorescence intensity of IMFD-70B/hSSTR5 (the feedback activation strain) was higher than that of the common activation strain at all SST concentrations tested. A similar result was obtained from the data at each optimal cultivation time (IMFD-70/hSSTR5 at 12 h and IMFD-70B/hSSTR5 at 18 h) (see Supplementary Fig. S2B). Moreover, compared with the GFP fluorescence induced by Ste2p in the IMFD-70 strain (the common activation strain), the level of hSSTR5 signaling was obviously lower, whereas the GFP fluorescence intensity of the Ste2p and hSSTR5 IMFD-70B strains (feedback activation strain) was equivalent (Fig. 4A). The EC_{50} value of the IMFD-70B/hSSTR5 strain was clearly improved as compared with that of the IMFD-70/hSSTR5 strain (from 55 to 8 nM). In addition, the advantage of IMFD-70B/hSSTR5 was supported by the fact that the EC_{50} value of the IMFD-70/hSSTR5 strain was almost similar to the value reported previously (109 nM) [11]. These results suggest that feedback signal activation compensates

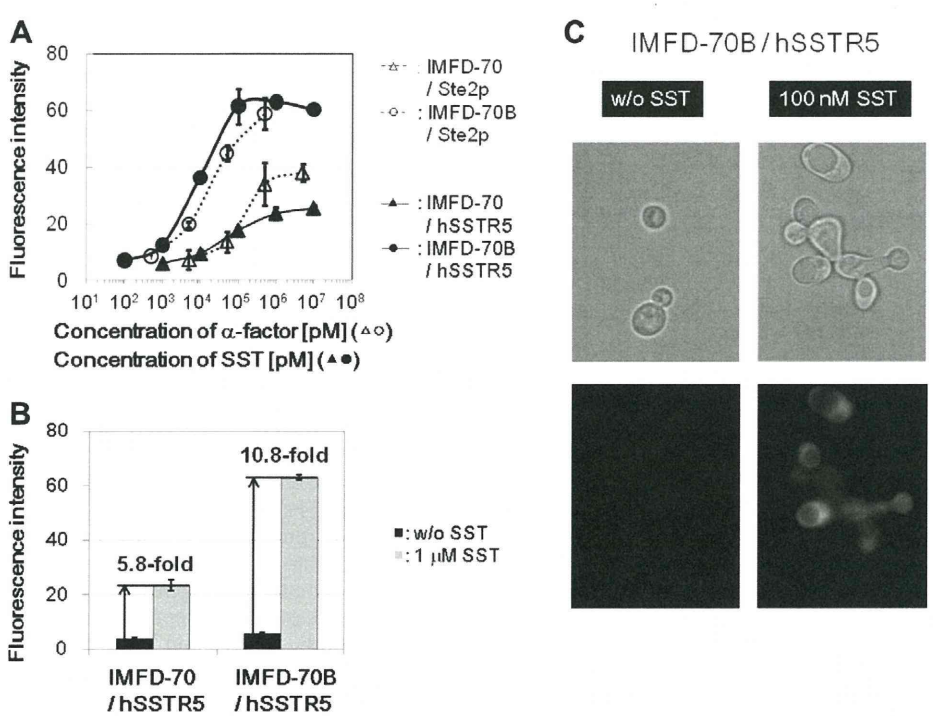

Fig.4. Fluorescence of a *GFP* reporter gene in response to agonist stimulation of common and feedback activation strains of yeast expressing hSSTR5. (A) Concentration–response curves of the common activation strain (IMFD-70/hSSTR5) and the feedback signal activation strain (IMFD-70B/hSSTR5) to the agonistic ligand SST. The dashed lines are overlays of the concentration–response curves of IMFD-70/Ste2p and IMFD-70B/Ste2p (data of Fig. 3B), which are included for comparative purposes. (B) Fluorescence of the *GFP* fluorescence reporter gene in IMFD-70/hSSTR5 and IMFD-70B/hSSTR5 with or without 1 μM SST stimulation. The fluorescence intensities are the average values of 10,000 cells. The results are presented as means ± standard deviations of three independent experiments. (C) Visualization of the green fluorescence of IMFD-70B/hSSTR5 with or without 100 nM SST. The upper photographs are differential interference contrast micrographs, and the lower photographs are fluorescence micrographs. w/o, without.

for inefficient receptor–G-protein coupling efficiency and significantly improves the sensitivity of agonist detection and the response to hSSTR5.

SST (1 μM) induced 5.8- and 10.8-fold increases over the signaling levels of unstimulated cells without agonistic ligands in the common and feedback activation strains, respectively (Fig. 4B). In addition, using a fluorescence microscope, we visually observed the changes in GFP fluorescence and morphology [29] in response to the SST-induced signal in the feedback activation strain (Fig. 4C). These results suggest that GFP fluorescence was specifically induced by agonists in the feedback activation strain and demonstrate the superiority and reliability of this approach for the detection of human GPCR agonists.

Conclusion

By expression of an artificial signal activator (Gβ) of the yeast G-protein signaling pathway, we have established a powerful approach for the detection of agonistic ligands of human GPCRs that are regarded as pharmaceutical and therapeutic targets. Using hSSTR5 as a model receptor, we demonstrated that feedback signal activation expands the detection limit for GPCR ligands and the maximum level of GPCR signaling in yeast. Our method is a reliable and versatile tool that could enhance the usefulness of yeast-based screening of agonistic ligands for a variety of human GPCRs.

Acknowledgments

This work was supported by a Research Fellowship for Young Scientists from the Japan Society for the Promotion of Science and, in part, by Special Coordination Funds for Promoting Science and Technology, Creation of Innovation Centers for Advanced Interdisciplinary Research Areas (Innovative Bioproduction Kobe), Ministry of Education, Culture, Sports, Science, and Technology (MEXT), Japan.

Appendix A. Supplementary data

Supplementary data associated with this article can be found, in the online version, at doi:10.1016/j.ab.2011.06.006.

References

[1] A.L. Hopkins, C.R. Groom, The druggable genome, Nat. Rev. Drug Discov. 1 (2002) 727–730.
[2] J. Giacomotto, L. Ségalat, High-throughput screening and small animal models: where are we?, Br J. Pharmacol. 160 (2006) 204–216.
[3] G.D. Stewart, C. Valant, S.J. Dowell, D. Mijaljica, R.J. Devenish, P.J. Scammells, P.M. Sexton, A. Christopoulos, Determination of adenosine A1 receptor agonist and antagonist pharmacology using *Saccharomyces cerevisiae*: implications for ligand screening and functional selectivity, J. Pharmacol. Exp. Ther. 331 (2009) 277–286.
[4] J. Minic, M. Sautel, R. Salesse, E. Pajot-Augy, Yeast system as a screening tool for pharmacological assessment of G-protein coupled receptors, Curr. Med. Chem. 12 (2005) 961–969.
[5] J.P. Manfredi, C. Klein, J.J. Herrero, D.R. Byrd, J. Trueheart, W.T. Wiesler, D.M. Fowlkes, J.R. Broach, Yeast α mating factor structure-activity relationship derived from genetically selected peptide agonists and antagonists of Ste2p, Mol. Cell. Biol. 16 (1996) 4700–4709.
[6] M.H. Pausch, M. Lai, E. Tseng, J. Paulsen, B. Bates, S. Kwak, Functional expression of human and mouse P2Y12 receptors in *Saccharomyces cerevisiae*, Biochem. Biophys. Res. Commun. 324 (2004) 171–177.
[7] E.V. Shusta, P.D. Holler, M.C. Kieke, D.M. Kranz, K.D. Wittrup, Directed evolution of a stable scaffold for T-cell receptor engineering, Nat. Biotechnol. 18 (2000) 754–759.
[8] M.J. Feldhaus, R.W. Siegel, L.K. Opresko, J.R. Coleman, J.M. Feldhaus, Y.A. Yeung, J.R. Cochran, P. Heinzelman, D. Colby, J. Swers, C. Graff, H.S. Wiley, K.D. Wittrup, Flow-cytometric isolation of human antibodies from a nonimmune *Saccharomyces cerevisiae* surface display library, Nat. Biotechnol. 21 (2003) 163–170.
[9] N. Fukuda, J. Ishii, S. Shibasaki, M. Ueda, H. Fukuda, A. Kondo, High-efficiency recovery of target cells using improved yeast display system for detection of protein–protein interactions, Appl. Microbiol. Biotechnol. 76 (2007) 151–158.
[10] G. Ladds, A. Goddard, J. Davey, Functional analysis of heterologous GPCR signalling pathways in yeast, Trends Biotechnol. 23 (2005) 367–373.
[11] S. Togawa, J. Ishii, A. Ishikura, T. Tanaka, C. Ogino, A. Kondo, Importance of asparagine residues at positions 13 and 26 on the amino-terminal domain of human somatostatin receptor subtype-5 in signalling, J. Biochem. 147 (2010) 867–873.
[12] N. Fukuda, J. Ishii, T. Tanaka, H. Fukuda, A. Kondo, Construction of a novel detection system for protein–protein interactions using yeast G-protein signaling, FEBS J. 276 (2009) 2636–2644.
[13] N. Fukuda, J. Ishii, T. Tanaka, A. Kondo, The competitor-introduced Gγ recruitment system, a new approach for screening affinity-enhanced proteins, FEBS J. 277 (2010) 1704–1712.
[14] J. Ishii, N. Fukuda, T. Tanaka, C. Ogino, A. Kondo, Protein–protein interactions and selection: yeast-based approaches that exploit guanine nucleotide-binding protein signaling, FEBS J. 277 (2010) 1982–1995.
[15] Y. Iguchi, J. Ishii, H. Nakayama, A. Ishikura, K. Izawa, T. Tanaka, C. Ogino, A. Kondo, Control of signalling properties of human somatostatin receptor subtype-5 by additional signal sequences on its amino-terminus in yeast, J. Biochem. 147 (2010) 875–884.
[16] C.B. Brachmann, A. Davies, G.J. Cost, E. Caputo, J. Li, P. Hieter, J.D. Boeke, Designer deletion strains derived from *Saccharomyces cerevisiae* S288C: A useful set of strains and plasmids for PCR-mediated gene disruption and other applications, Yeast 14 (1998) 115–132.
[17] N. Fukuda, J. Ishii, A. Kondo, Gγ recruitment system incorporating a novel signal amplification circuit to screen transient protein-protein interactions, FEBS J. (2011), doi:10.1111/j.1742-4658.2011.08232.x.
[18] J. Ishii, K. Izawa, S. Matsumura, K. Wakamura, T. Tanino, T. Tanaka, C. Ogino, H. Fukuda, A. Kondo, A simple and immediate method for simultaneously evaluating expression level and plasmid maintenance in yeast, J. Biochem. 145 (2009) 701–708.
[19] D. Gietz, A. St. Jean, R.A. Woods, R.H. Schiestl, Improved method for high efficiency transformation of intact yeast cells, Nucleic Acids Res. 20 (1992) 1425.
[20] S.N. Ho, H.D. Hunt, R.M. Horton, J.K. Pullen, L.R. Pease, Site-directed mutagenesis by overlap extension using the polymerase chain reaction, Gene 77 (1989) 51–59.
[21] J. Ishii, T. Tanaka, S. Matsumura, K. Tatematsu, S. Kuroda, C. Ogino, H. Fukuda, A. Kondo, Yeast-based fluorescence reporter assay of G-protein-coupled receptor signalling for flow cytometric screening: *FAR1* -disruption recovers loss of episomal plasmid caused by signalling in yeast, J. Biochem. 143 (2008) 667–674.
[22] S. Nomoto, N. Nakayama, K. Arai, K. Matsumoto, Regulation of the yeast pheromone response pathway by G protein subunits, EMBO J. 9 (1990) 691–696.
[23] M. Whiteway, L. Hougan, D.Y. Thomas, Overexpression of the STE4 gene leads to mating response in haploid *Saccharomyces cerevisiae*, Mol. Cell. Biol. 10 (1990) 217–222.
[24] K.L. Clark, D. Dignard, D.Y. Thomas, M. Whiteway, Interactions among the subunits of the G protein involved in *Saccharomyces cerevisiae* mating, Mol. Cell. Biol. 13 (1993) 1–8.
[25] J. Ishii, S. Matsumura, S. Kimura, K. Tatematsu, S. Kuroda, H. Fukuda, A. Kondo, Quantitative and dynamic analyses of G-protein-coupled receptor signaling in yeast using Fus1, enhanced green fluorescence protein (EGFP), and His3 fusion protein, Biotechnol. Prog. 22 (2006) 954–960.
[26] T. Saito, N. Iwata, S. Tsubuki, Y. Takaki, J. Takano, S.M. Huang, T. Suemoto, M. Higuchi, T.C. Saido, Somatostatin regulates brain amyloid β peptide Aβ42 through modulation of proteolytic degradation, Nat. Med. 11 (2005) 434–439.
[27] S.W. Lamberts, W.W. de Herder, E.P. Krenning, J.C. Reubi, A role of (labeled) somatostatin analogs in the differential diagnosis and treatment of Cushing's syndrome, J. Clin. Endocrinol. Metab. 78 (1994) 17–19.
[28] A. Ben-Shlomo, S. Melmed, Somatostatin agonists for treatment of acromegaly, Mol. Cell. Endocrinol. 286 (2008) 192–198.
[29] L. Yu, M. Qi, M.A. Sheff, E.A. Elion, Counteractive control of polarized morphogenesis during mating by mitogen-activated protein kinase Fus3 and G1 cyclin-dependent kinase, Mol. Biol. Cell 19 (2008) 1739–1752.

Int. J. Radiation Oncology Biol. Phys., Vol. ■, No. ■, pp. 1–6, 2011

0360-3016/$ - see front matter

ELSEVIER

doi:10.1016/j.ijrobp.2011.04.052

CLINICAL INVESTIGATION

LONG-TERM OUTCOME AND PATTERNS OF FAILURE IN PRIMARY OCULAR ADNEXAL MUCOSA-ASSOCIATED LYMPHOID TISSUE LYMPHOMA TREATED WITH RADIOTHERAPY

Naoki Hashimoto, M.D.,* Ryohei Sasaki, M.D.,* Hideki Nishimura, M.D.,* Kenji Yoshida, M.D.,* Daisuke Miyawaki, M.D.,* Masao Nakayama, M.S.,* Kazuyuki Uehara, M.S.,* Yoshiaki Okamoto, M.D.,* Yasuo Ejima, M.D.,* Atsushi Azumi, M.D.,† Toshimitsu Matsui, M.D.,‡ and Kazuro Sugimura, M.D.*

Divisions of *Radiation Oncology, †Ophthalmology, and ‡Hematology, Kobe University Graduate School of Medicine, Hyogo, Japan

Purpose: To evaluate the long-term treatment outcome and disease behavior of primary ocular adnexal MALT (mucosa-associated lymphoid tissue) lymphoma (POAML) after treatment with radiotherapy.
Methods and Materials: Seventy-eight patients (42 male, 36 female) diagnosed with stage I POAML between 1991 and 2010 at Kobe University Hospital were included. The median age was 60 years (range, 22–85 years). The median radiation dose administered was 30.6 Gy. Rituximab-based targeted therapy and/or chemotherapy was performed in 20 patients (25.6%). Local control (LC), recurrence-free survival (RFS), and overall survival (OS) rates were calculated using the Kaplan-Meier method.
Results: The median follow-up duration was 66 months. Major tumor sites were conjunctiva in 37 patients (47.4%), orbita in 29 (37.2%), and lacrimal glands in 12 (15.4%). The 5- and 10-year OS rates were 98.1% and 95.3%, respectively. The 5- and 10-year LC rates were both 100%, and the 5- and 10-year RFS rates were 88.5% and 75.9%, respectively. Patients treated with a combination of radiotherapy and targeted therapy and/or chemotherapy had a trend for a better RFS compared with those treated with radiotherapy alone (p = 0.114). None developed greater than Grade 2 acute morbidity. There were 14 patients who experienced Grade 2 morbidities (cataract: 14; retinal disorders: 7; dry eye: 3), 23 patients who had Grade 3 morbidities (cataract: 23; dry eye: 1), and 1 patient who had Grade 4 glaucoma.
Conclusions: Radiotherapy for POAML was shown to be highly effective and safe for LC and OS on the basis of long-term observation. The absence of systemic relapse in patients with combined-modality treatment suggests that lower doses of radiation combined with targeted therapy may be worth further study. © 2011 Elsevier Inc.

MALT lymphoma, Ocular adnexal lymphoma, Radiotherapy, Pattern of failure.

INTRODUCTION

Since the first description by Isaacson and Wright in 1983, extranodal marginal zone B-cell lymphoma of mucosa-associated lymphoid tissue (MALT) lymphoma has been recognized as a distinct entity of low-grade B-cell lymphoma; it is described in the revised European-American lymphoma (REAL) classification and also in the more-recent classification by the World Health Organization (WHO) (1–3). Malignant lymphoma arising in the ocular adnexa is a rare disorder, and previous reports have indicated that these lymphomas account for approximately 8% of all extranodal lymphomas (4). Several reports have indicated that the majority of lymphomas in the ocular adnexa are of MALT type (5–9). It was reported that histology, according to the REAL or WHO classification, could be used to accurately predict the prognosis of patients with lymphomas in the ocular adnexa and that patients with MALT-type lymphomas have a more favorable prognosis than those with lymphomas of different histology (6–9).

Mucosa-associated lymphoid tissue lymphomas have generally been believed to follow a relatively indolent course and show a tendency to remain localized within their original environment for a long period (10, 11). First-line treatment options include radiotherapy (standard), chemotherapy, or

Reprint requests to: Ryohei Sasaki, M.D., Ph.D., Kobe University Graduate School of Medicine, Division of Radiation Oncology, 7-5-2 Kusunokicho, Chuouku, Kobe City, Hyogo 650-0017, Japan. Tel: (+81) 78-3826104; Fax: (+81) 78-3826129; E-mail: rsasaki@med.kobe-u.ac.jp

Supported by Grants-in-Aid and Grants 21249066, 21591609, and 22591384 for Scientific Research from the Ministry of Education, Culture, Sports, Science and Technology of Japan.

Y. Okamoto's present address: Department of Radiation Oncology, Osaka Police Hospital, Tennoji, Japan.
Y. Ejima's present address: Department of Radiology, Dokkyo Medical University, Tochigi, Japan.

Conflict of interest: none.
Received Feb 9, 2011, and in revised form April 14, 2011. Accepted for publication April 19, 2011.

even a wait-and-see policy in certain clearly defined patients (12). Therefore, there has been no consensus regarding the initial management of POAML to date; radiotherapy has been generally considered the most effective treatment for localized disease (13–19). Although results for local control (LC) by radiotherapy were satisfying, disease progression occurred in a fraction of patients. There have been few analyses of disease progression and death in patients with POAML (19–22).

After reporting our treatment outcomes for POAML treated with radiotherapy alone (23), we have started another protocol of radiotherapy combined with rituximab-based targeted therapy and/or chemotherapy. Several investigators demonstrated that although high LC was achieved by the radiotherapy for POAML, patterns of systemic relapse have not been elucidated (13, 18, 24, 25). The purposes of this analysis were to determine the long-term follow-up results of POAML patients treated with radiotherapy at our institution, to analyze patterns of failure of POAML, and to evaluate the outcome of patients treated with the radiotherapy combined with targeted therapy.

METHODS AND MATERIALS

Patients

Seventy-eight consecutive patients with histologically proven stage I ocular adnexal MALT lymphoma treated with radiotherapy at Kobe University Hospital between March 1991 and June 2010 were retrospectively reviewed. The retrospective review and the use of the clinical data followed the guidelines of the institutional ethics board of Kobe University Hospital, derived from the ethical guidelines for epidemiologic research by the Ministry of Education, Culture, Sports, Science and Technology and Ministry of Health, Labor and Welfare of Japan. The median age was 60 years (range, 22–85 years). There were 42 male (53.8%) and 36 female (46.2%) patients. A diagnosis of MALT lymphoma was established by biopsy or a surgical resection sample, and hemotoxylin and eosin–stained microscopic examination and immunohistochemical staining for CD20, CD3, CD5, and cyclinD1 were performed to exclude other pathologic subtypes.

Staging workup

Before starting the initial treatment, a physical examination, chest X-ray, complete blood count, MRI of both orbits, CT of the neck, chest, abdomen, and pelvis, and bone marrow biopsy were performed on all patients. Positron emission tomography, bone scan, or gallium scan was performed selectively. Tumors that were classified as stage IE in this study were unilateral or bilateral tumors without other lesions outside the orbit.

Treatment

Treatment policies differed according to treatment periods. From 1991 to 2004, a single modality of radiotherapy was used. From May 2000, a single modality of radiotherapy was mainly adopted, but a combination of radiotherapy and targeted therapy and/or chemotherapy was used in 3 patients. After 2004, a combination of radiotherapy and chemotherapy was used in 17 of 30 patients (56.7%). A total of 58 of the 78 patients (74.4%) were treated by radiotherapy alone, whereas the other 20 patients (25.6%) received targeted therapy or chemotherapy followed by radiotherapy. Among those treated with a combination of therapies, 17 patients had three or four courses of rituximab, 2 patients had two or three courses of CHOP (cyclophosphamide, doxorubicin, vincristine, and prednisone), and 1 patient had an R-CHOP (rituximab and CHOP) regimen.

The radiation dose and schedule varied according to the treatment periods. Before February 2000, various radiation doses and schedules (range, 30–50 Gy in 18–25 fractions) were used in 17 patients. Since March 2000, a single schedule of 30.6 Gy in 17 fractions was adopted in the majority of patients (55 patients), with the exception of 3 patients who were treated with 32.4 Gy in 18 fractions (1 patient) or 36 Gy in 20 fractions (2 patients) (Table 1). In total, the median dose was 30.6 Gy. Forty-eight patients with disease at the conjunctiva, eyelid, and lacrimal gland were treated with electron beams (4–15 MeV) from a single anterior field. A cylindrical lead lens block, approximately 4 mm thick and 10 mm in diameter, was used with 4–15-MeV electron beams in 41 of the 48 patients (85.4%). The lens block was placed directly on the cornea after topical anesthesia. A 4-MeV photon beam was used in the other 30 patients (38.5%) for tumors located in the orbital soft tissue. Dose coverage and distribution of the tumor and surrounding critical structures were carefully considered with and without the use of a lens block, wedge, or bolus.

Follow-up evaluation and statistical analyses

In the follow-up evaluations, local and disease progression were evaluated every year using the same method as in the initial staging, with the exception of bone marrow biopsy. Morbidities were evaluated and re-graded by the ophthalmologist according to the Common Terminology Criteria for Adverse Events (CTCAE) version 3.0. Local control, recurrence-free survival (RFS), overall survival (OS), and cause-specific survival (CSS) were analyzed statistically in all patients. Recurrence-free survival was calculated from the first day of radiotherapy to the date of first documented relapse or the date of death. Overall survival was calculated from the first day of radiotherapy to the date of death or the date of last follow-up. Curves for each survival type were calculated using Kaplan-Meier estimates. Statistical significance was tested by the log–rank test.

RESULTS

Tumor locations and characteristics

The tumor was located in the eyelid or conjunctiva in 37 patients (47.4%), the orbita in 29 patients (37.2%), and in the lacrimal gland in 12 patients (15.4%). Sixty-four patients

Table 1. Treatment methods in patients with POAML (n = 78)

Parameter	n	%
Initial treatment		
Radiotherapy alone	58	74.4
Targeted therapy and/or chemotherapy followed by radiotherapy	20	25.6
CHOP	2	2.6
Rituximab and CHOP	1	1.3
Rituximab	17	21.7
Radiation dose (median, 30.6 Gy)		
36–50 Gy/18–25 fractions	17	21.8
30–32.4 Gy/15–18 fractions	61	78.2
Radiation source		
6–12-MeV electron beam	48	61.5
4-MV photon beam	30	38.5

Abbreviations: POAML = primary ocular adnexal MALT (mucosa-associated lymphoid tissue) lymphoma; CHOP = cyclophosphamide, doxorubicin, vincristine and prednisone.

(82.1%) had unilateral lesions, and 14 patients (17.9%) had bilateral lesions.

Survival and causes of death

The median follow-up duration was 66 months (range, 3–234 months). Five-year and 10-year OS rates were 98.1% and 95.3%, respectively, and the 5- and 10-year CSS rates were both 100% (Fig. 1). None died of the disease; the deaths of 2 patients (2.6%) were from non–lymphoma-related causes.

LC, disease progression, and patterns of recurrence

There was no case that recurred locally, and therefore the 5- and 10-year LC rates were both 100% (Fig. 2). The 5- and 10-year RFS rates were 88.5% and 75.9%, respectively (Fig. 3). Patients treated with radiotherapy combined with targeted therapy and/or chemotherapy (5- and 10-year rates both 100%) showed a trend for better RFS than those who were treated with a single modality of radiotherapy (5- and 10-year rates: 85.3% and 71.1%, respectively; $p = 0.114$) (Fig. 4). Ten patients (12.8%) relapsed somewhere other than the original tumors (distant regions) (Table 2). The median duration to distant relapse was 33 months. Five patients (6.4%) relapsed at the contralateral orbit. Of the other 5 patients, 2 relapsed at nodes in the abdomen and the neck, 2 relapsed in the stomach, and 1 patient relapsed in the parenchyma of the lung. No patient showed the histology of a transformed high-grade lymphoma. Eight of the relapsed patients underwent a second-line therapy, and another 2 patients were observed without a second-line therapy (Table 2). One patient died from non–lymphoma-related causes. Notably, 20 patients (25.6%) treated with radiotherapy and targeted therapy and/or chemotherapy did not experience any distant or contralateral orbital recurrence (Table 3).

Morbidity

Any symptom related to the radiotherapy that occurred during from initial day to 1 month after completion of radiotherapy was defined as acute morbidity with reference to CTCAE version 3.0. Fifty-two patients (66.7%) had Grade 1 acute morbidity, and only 6 (7.7%) had Grade 2 acute morbidity. No patients developed greater than Grade 2 acute morbidity; the most frequent morbidities were mild conjunctivitis, excessive tearing or dryness, and periorbital erythema or edema.

There were 14 patients who experienced Grade 2 morbidities (cataract: 14; retinal disorders: 7; dry eye: 3), 23 patients who had Grade 3 morbidities (cataract: 23; dry eye: 1), and 1 patient who had Grade 4 glaucoma. Cataracts (Grade 3) were observed at a median 38 months (range, 9–88 months) after radiotherapy.

Risk factors for morbidity were retrospectively evaluated. For occurrence of retinal disorders (greater than Grade 2), the radiation dose was a significant risk factor (1.6% in patients treated with 30–32.4 Gy vs. 35.3% in patients treated with 36–40 Gy; $p < 0.0001$). Grade 2 retinopathies were observed in 5 patients, and a Grade 2 macular hole was observed in a patient who also developed a Grade 3 dry eye. Notably, these 6 patients received 36–40 Gy. The

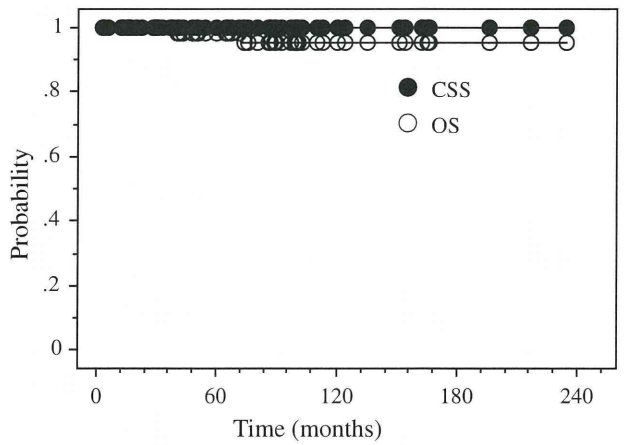

Fig. 1. Kaplan-Meier curves of cause-specific survival (CSS) and overall survival (OS) in patients with primary ocular adnexal MALT (mucosa-associated lymphoid tissue) lymphoma ($n = 78$) (10-year CSS rate: 100%; 5- and 10-year OS rates: 98.1% and 95.3%, respectively).

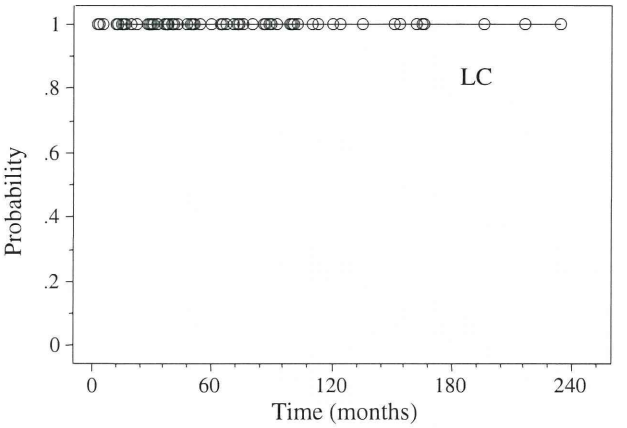

Fig. 2. Kaplan-Meier curve of local control (LC) in patients with primary ocular adnexal MALT (mucosa-associated lymphoid tissue) lymphoma ($n = 78$) (10-year LC rate: 100%).

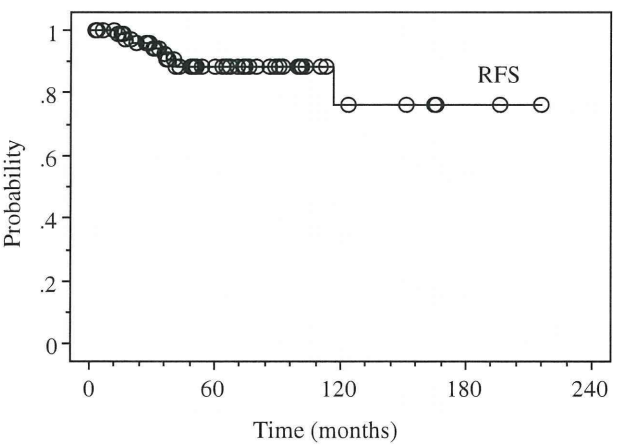

Fig. 3. Kaplan-Meier curve of recurrence-free survival (RFS) in patients with primary ocular adnexal MALT (mucosa-associated lymphoid tissue) lymphoma ($n = 78$) (5- and 10-year RFS rates: 88.5% and 75.9%, respectively).

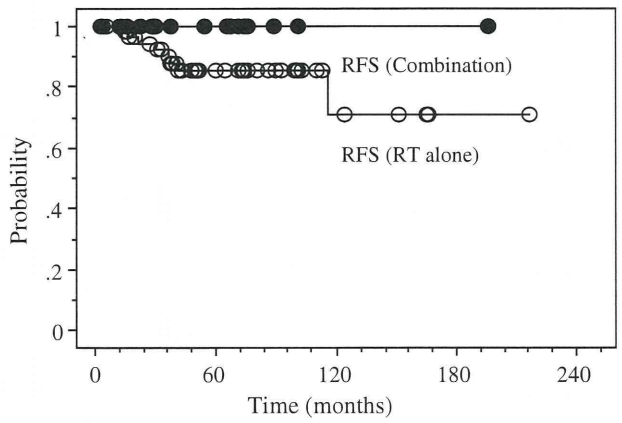

Fig. 4. Comparison of recurrence-free survival (RFS) in patients treated with a combination of targeted therapy and/or chemotherapy and radiotherapy (n = 20) and patients treated with radiation alone (n = 58) (10-year RFS rate of combination therapy: 100%, vs. 5- and 10-year RFS rates of radiotherapy alone: 85.3% and 71.1%, respectively).

other patient, who received 30.6 Gy, developed a retinal embolism (Grade 3). Grade 3 cataracts occurred in 13 of 61 patients (21.3%) treated with <36 Gy and in 10 of 17 patients (58.8%) treated with ≥36 Gy (p = 0.0027). A lens-sparing technique was used in 44 of the 78 patients (56.4%) whose tumor locations were conjunctiva or lacrimal gland. Nineteen of the 34 patients (55.9%) without lens shielding developed a Grade 3 cataract, whereas 4 of the 44 patients (9.1%) with lens shielding developed a cataract ($p < 0.001$). Although the lens-sparing technique was useful to avoid cataract, it was inadequate to use in case that tumor location was the orbita. Visual acuity of these 23 patients was successfully saved by cataract extraction. As a result, to avoid severe morbidities, a 30.6-Gy or lesser dose and the lens-sparing technique (restricted to the tumor at conjunctiva or lacrimal gland) might be recommended.

Prognostic factors

Several factors were evaluated for prognostic significance of RFS. Among them, combinations with targeted therapy and/or chemotherapy showed a trend for better RFS; however, it was not significant (with targeted therapy and/or chemotherapy [n = 20] vs. without targeted therapy and/or chemotherapy [n = 58], p = 0.114). Other factors, such as tumor location (conjunctiva [n = 37] vs. orbita [n = 29] vs. lacrimal gland [n = 12], p = 0.315), age (≤ 60 [n = 36] vs. > 61 [n = 42], p = 0.723), gender (male [n = 42] vs. female [n = 36], p = 0.201), and radiation dose (≤32.4 Gy [n = 61] vs. >36 Gy [n = 17], p = 0.575), were not significant.

DISCUSSION

The present study summarizes our institution's experience in a large cohort of POAML patients with long-term follow-up. Our study not only confirmed some of the previously reported observations but also elucidated patterns of failure and characteristics of Stage I POAML.

Excellent LC was achieved in our series of patients with Stage I POAML using moderate doses of 30 Gy. Previously, Fung *et al.* (26) reported that, in their series, the local relapse rate was higher in patients who received <30.6 Gy. Many authors have concluded that low-grade orbital lymphoma, including MALT, could be successfully controlled by radiation doses in the range of 25–34 Gy. Tsang and coworkers (13, 25) reported that, for LC, results from the use of a slightly lower dose of 25 Gy (in 10–15 fractions) in orbital lymphomas remained excellent. In our study, a median dose of 30.6 Gy was used, and 100% LC has been achieved. Therefore, the optimal radiation dose seems still to be a matter for discussion, and radiotherapy has remained the assumed standard for the initial treatment of POAML.

For localized MALT lymphoma, despite offering excellent LC, radiotherapy might not be useful in preventing systemic relapses, occurring in 5–45% of patients (8, 13, 18, 19, 22–31). Tsang *et al.* (13) demonstrated that although excellent LC can be achieved with infrequent long-term toxicity by a single modality of radiotherapy, the risk of relapse in distant extranodal sites remains a significant problem. Bayraktar *et al.* (31) demonstrated that patients with Stage I POAML face a continuous risk of distant relapse, which increases from an estimated cumulative progression rate of 17.8% at 5 years to 41.5% at 10 years. Therefore, the focus of POAML management may not only include LC but also

Table 2. Details of POAML patients who relapsed after radiotherapy

Patient	Age/ gender	Initial site	Radiation dose (Gy)	Relapse site	Duration to relapse (mo)	Treatment for relapse
1	40/F	Conjunctiva	30.6	Contralateral conjunctiva	13	Radiotherapy
2	73/M	Conjunctiva	36	Stomach	27	Endoscopic mucosal resection
3	49/F	Conjunctiva	30	Contralateral conjunctiva	116	Radiotherapy
4	63/F	Lacrimal gland	30.6	Contralateral conjunctiva	21	Rituximab and chemotherapy and radiotherapy
5	49/M	Lacrimal gland	40	Lymph nodes	30	Rituximab and chemotherapy
6	40/F	Lacrimal gland	30	Stomach	41	Radiotherapy
7	77/M	Orbit	36	Lymph nodes and spleen	17	Rituximab and chemotherapy
8	54/M	Orbit	40	Contralateral orbit	36	Rituximab and chemotherapy
9	72/F	Orbit	30.6	Contralateral orbit	37	No treatment (observation)
10	50/F	Orbit	40	Lung parenchyma	86	No treatment (observation)

Abbreviations: F = female; M = male. Other abbreviation as in Table 1.

Table 3. Patterns of relapses in patients with stage I-II POAML treated with radiotherapy

First author (reference)*	Reported year	*N*	Clinical stage (I/II/III/IV)	Median follow-up (mo)	Radiation dose (Gy)	No. of patients			
							Sites of relapsed tumors		
						Total	Local	Contralateral orbit	Distant
Tsang (13)	2003	30	I-II:30/0/0	60	25	8	2	3	3
Uno (18)	2003	50	50/0/0/0	46	36	6	3	0	3
Suh (32)	2006	48	46/1/0/1	70	30.6	3	3	0	0
Ejima (23)	2006	42	42/0/0/0	48	30.6	8	0	4	4
Nam (27)	2009	66	66/0/0/0	50	30	6	3	2	3
Goda (25)	2010	71	I-II:71/0/0	89	25	18	3	5	11†
Son (28)	2010	46	46/0/0/0	32	30.6	2	0	1	1
Bayraktar (31)	2011	70	70/0/0/0	60	30.6	14	6	NA	10
Total		423				65 (15.4)	20(4.7)	15 (3.5)	35(8.3)
Present study	2011	58	58/0/0/0	73.5	RT: 30.6	10 (17.2)	0	5 (8.6)	5 (8.6)
		20	20/0/0/0	45.5	RT: 30.6 + rituximab	0	0	0	0
Total	2011	78	78/0/0/0	66		(12.8)	0	(6.4)	(6.4)

Abbreviation: RT = radiotherapy. Other abbreviation as in Table 1.
Values in parentheses are percentages.
* The listed articles all included outcome of RT for Stage I–II POAML. Other articles contained various histologic orbital tumors, or articles included more than 10% stage III–IV MALT disease were not included.
† Extraorbital recurrence.

systemic disease control. However, the significance of chemotherapy for systemic disease control has not been widely accepted in the initial treatment of MALT lymphoma. A large, retrospective study conducted by the International Extra Nodal Lymphoma Study Group analyzed the results of 180 patients, including patients with Stage I–IV MALT lymphoma, and did not find any difference in the clinical outcome between initial localized treatment approaches with systemic chemotherapy (29). The efficacy of the combination of radiotherapy and chemotherapy has not been fully investigated. Goda *et al.* (25) reported that the initial role of chemotherapy could not be determined in their series; however, they suggested that it must have contributed to control of the disease because all patients had partial or complete responses from chemotherapy before the initiation of radiotherapy. We searched for all articles published between 2000 and 2011 that included the outcome in patients with Stage I–II POAML (Table 3); previous investigators reported similar risks of local relapse, contralateral relapse, and distant relapses when patients were treated with radiation alone (12, 17, 22, 24, 26, 27, 32). In our series, although the cohort who received radiotherapy alone had similar pattern of relapse, notably, the outcome of the other cohort treated with combined radiotherapy and rituximab showed decreased systemic relapse (Table 3).

The best way to treat POAML should be considered carefully to avoid overtreatment. A combination of reduced-dose radiotherapy and rituximab could be proposed as an optimal treatment for POAML. Several examples in the treatment of lymphoma or medulloblastoma using a strategy of reduced radiation doses with chemotherapy have been investigated (33–36). Conversely, there are few data regarding how much the dose could be reduced safely in the combination. In our series, the protocol consisting of 30.6 Gy radiotherapy combined with rituximab successfully decreased risks of systemic relapse. However, it remains unknown whether doses less than 30.6 Gy might keep satisfying LC and whether those doses lead to reduced risks of morbidity, including cataract. Therefore, future clinical trials seem to be necessary to set optimal doses in the strategy of combination therapy.

In conclusion, radiotherapy for POAML was highly effective and safe for LC and OS. The absence of systemic relapse in patients with combined-modality treatment suggests that lower doses of radiation combined with targeted therapy may be worth further study.

REFERENCES

1. Isaacson PG, Wright D. Malignant lymphoma of mucosa-associated lymphoid tissue: A distinctive type of B-cell lymphoma. *Cancer* 1983;52:1410–1416.
2. Harris NL, Jaffe ES, Stein H, *et al.* A revised European-American classification of lymphoid neoplasm: A proposal from the International Lymphoma Study Group. *Blood* 1994; 84:1361–1392.
3. Isaacson PG, Muller-Hermelink HK, Piris MA, *et al.* Extranodal marginal zone B-cell lymphoma of mucosa-associated lymphoid tissue (MALT lymphoma). In: Jaffe ES, Harris NI, Stein H, *et al.*, editors. World Health Organization classification of tumors. Pathology genetics of haematopoietic and lymphoid tissue. Lyon, France: IARC Press; 2001. p. 157–160.

4. Freeman C, Berg JW, Cutler SJ. Occurrence and prognosis of extranodal lymphomas. *Cancer* 1972;29:252–260.
5. White WL, Ferry JA, Harris NL, *et al.* Ocular adnexal lymphoma: A clinicopathologic study with identification of lymphomas of mucosa-associated lymphoid tissue type. *Ophthalmology* 1995;102:1994–2006.
6. Nakata M, Matsuno Y, Katsumata N, *et al.* Histology according to the revised European-American Lymphoma classification significantly predicts the prognosis of ocular adnexal lymphoma. *Leuk Lymphoma* 1999;32:533–543.
7. Cho EY, Han JJ, Ree HJ, *et al.* Clinicopathologic analysis of ocular adnexal lymphomas: Extranodal marginal zone B-cell lymphoma constitutes the vast majority of ocular lymphomas among Koreans and affects younger patients. *Am J Hematol* 2003;73:87–96.
8. Jenkins C, Rose GE, Bunce C, *et al.* Histological features of ocular adnexal lymphoma (REAL classification) and their association with patient morbidity and survival. *Br J Ophthalmol* 2000;84:907–913.
9. Auw-Haedrich C, Coupland SE, Kapp A, *et al.* Long term outcome of ocular adnexal lymphoma subtyped according to the REAL classification. *Br J Ophthalmol* 2001;85:63–69.
10. Thieblemont C, Bastion Y, Berger F, *et al.* Mucosa-associated lymphoid tissue gastrointestinal and nongastrointestinal lymphoma behavior. *J Clin Oncol* 1997;15:1624–1630.
11. Thieblemont C, Berger F, Dumontet C, *et al.* Mucosa-associated lymphoid tissue lymphoma is a disseminated disease in one third of 158 patients analyzed. *Blood* 2000;95: 802–806.
12. Song EK, Kim SY, Kim TM, *et al.* Efficacy of chemotherapy as a first-line treatment in ocular adnexal extranodal marginal zone B-cell lymphoma. *Ann Oncol* 2008;19:242–246.
13. Tsang RW, Gospodarowicz MK, Pintilie M, *et al.* Localized mucosa-associated lymphoid tissue lymphoma treated with radiation therapy has excellent clinical outcome. *J Clin Oncol* 2003;21:4157–4164.
14. Tsang RW, Gospodarowicz MK, Pintilie M, *et al.* Stage I and II MALT lymphoma: Results of treatment with radiotherapy. *Int J Radiat Oncol Biol Phys* 2001;50:1258–1264.
15. Le QT, Eulau SM, George TI, *et al.* Primary radiotherapy for localized orbital MALT lymphoma. *Int J Radiat Oncol Biol Phys* 2002;52:657–663.
16. Bhatia S, Paulino AC, Buatti JM, *et al.* Curative radiotherapy for primary orbital lymphoma. *Int J Radiat Oncol Biol Phys* 2002;54:818–823.
17. Martinet S, Ozsahin M, Belkacemi Y, *et al.* Outcome and prognostic factors in orbital lymphoma: A rare cancer network study on 90 consecutive patients treated with radiotherapy. *Int J Radiat Oncol Biol Phys* 2003;55:892–898.
18. Uno T, Isobe K, Shikama N, *et al.* Radiotherapy for extranodal, marginal zone, B-cell lymphoma of mucosa-associated lymphoid tissue originating in the ocular adnexa. *Cancer* 2003; 98:865–871.
19. Tanimoto K, Kaneko A, Suzuki S, *et al.* Primary ocular adnexal MALT lymphoma: A long-term follow-up study of 114 patients. *Jpn J Clin Oncol* 2007;37:337–344.
20. Lee JL, Kim MK, Lee KH, *et al.* Extranodal marginal zone B-cell lymphomas of mucosa-associated lymphoid tissue type of the orbit and ocular adnexa. *Ann Hematol* 2005;84: 13–18.
21. Charlotte F, Doghmi K, Cassoux N, *et al.* Ocular adnexal marginal zone B cell lymphoma: A clinical and pathologic study of 23 cases. *Virchows Arch* 2005;2:1–11.
22. Raderer M, Streubel B, Woehrer S, *et al.* High relapse rate in patients with MALT lymphoma warrants lifelong follow-up. *Clin Cancer Res* 2005;11:3349–3352.
23. Ejima Y, Sasaki R, Okamoto Y, *et al.* Ocular adnexal mucosa associated lymphoid tissue lymphoma treated with radiotherapy. *Radiother Oncol* 2006;78:6–9.
24. Fung CY, Tarbell NJ, Lucarelli MJ, *et al.* Ocular adnexal lymphoma: Clinical behavior of distinct world health organization classification subtypes. *Int J Radiat Oncol Biol Phys* 2003;57: 1382–1391.
25. Goda JS, Gospodarowicz M, Pintilie M, *et al.* Long-term outcome in localized extranodal mucosa-associated lymphoid tissue lymphomas treated with radiotherapy. *Cancer* 2010;116: 3815–3824.
26. Hasegawa M, Kojima M, Shioya M, *et al.* Treatment results of radiotherapy for malignant lymphoma of the orbit and histopathologic review according to the WHO classification. *Int J Radiat Oncol Biol Phys* 2003;57:172–176.
27. Nam H, Ahn YC, Kim YD, *et al.* Prognostic significance of anatomic subsites: Results of radiation therapy for 66 patients with localized orbital marginal zone B cell lymphoma. *Radiother Oncol* 2009;90:236–241.
28. Son SH, Choi BO, Kim GW, *et al.* Primary radiation therapy in patients with localized orbital marginal zone B-cell lymphoma of mucosa-associated lymphoid tissue (MALT Lymphoma). *Int J Radiat Oncol Biol Phys* 2010;77:86–91.
29. Zucca E, Conconi A, Pedrinis E, *et al.* Nongastric marginal zone B-cell lymphoma of mucosa-associated lymphoid tissue. *Blood* 2003;101:2489–2495.
30. Wenzel C, Fiebiger W, Dieckmann K, *et al.* Extranodal marginal zone B-cell lymphoma of mucosa-associated lymphoid tissue of the Head and Neck Area. *Cancer* 2003;97:2236–2241.
31. Bayraktar S, Bayraktar UD, Stefanovic A, *et al.* Primary ocular adnexal mucosa-associated lymphoid tissue lymphoma (MALT): Single institution experience in a large cohort of patients. *Br J Haematol* 2011;152:72–80.
32. Suh CO, Shim SJ, Lee SW, *et al.* Orbital marginal zone B-cell lymphoma of MALT: Radiotherapy results and clinical behavior. *Int J Radiat Oncol Biol Phys* 2006;65:228–233.
33. Engert A, Plütschow A, Eich HT, *et al.* Reduced treatment intensity in patients with early-stage Hodgkin's lymphoma. *N Engl J Med* 2010;363:640–652.
34. Shah GD, Yahalom J, Correa DD, *et al.* Combined immunochemotherapy with reduced whole-brain radiotherapy for newly diagnosed primary CNS lymphoma. *J Clin Oncol* 2007;25: 4730–4735.
35. Oyharcabal-Bourden V, Kalifa C, Gentet JC, *et al.* Standard-risk medulloblastoma treated by adjuvant chemotherapy followed by reduced-dose craniospinal radiation therapy: A French Society of Pediatric Oncology Study. *J Clin Oncol* 2005;23:4726–4734.
36. Merchant TE, Kun LE, Krasin MJ, *et al.* Multi-institution prospective trial of reduced-dose craniospinal irradiation (23.4 Gy) followed by conformal posterior fossa (36 Gy) and primary site irradiation (55.8 Gy) and dose-intensive chemotherapy for average-risk medulloblastoma. *Int J Radiat Oncol Biol Phys* 2008;70:782–787.

J Gastroenterol (2011) 46:913–920
DOI 10.1007/s00535-011-0398-6

ORIGINAL ARTICLE—LIVER, PANCREAS, AND BILIARY TRACT

The effectiveness of particle radiotherapy for hepatocellular carcinoma associated with inferior vena cava tumor thrombus

Shohei Komatsu · Takumi Fukumoto · Yusuke Demizu · Daisuke Miyawaki · Kazuki Terashima · Yasue Niwa · Masayuki Mima · Osamu Fujii · Ryohei Sasaki · Isamu Yamada · Yuichi Hori · Yoshio Hishikawa · Mitsuyuki Abe · Yonson Ku · Masao Murakami

Received: 20 August 2010 / Accepted: 8 March 2011 / Published online: 23 April 2011

Abstract
Background The prognosis of patients who have hepatocellular carcinoma (HCC) associated with inferior vena cava tumor thrombus (IVCTT) is very poor, and effective treatment modalities are extremely limited. The objective of this study was to determine the therapeutic efficacy of particle radiotherapy for HCC with IVCTT.
Methods Between June 2001 and January 2009, 16 evaluable patients who had HCC with IVCTT were treated with particle radiotherapy. They were divided into 2 groups: 6 were treated with curative intent; 10 with palliative intent. The local tumor control rates, overall survival rates, and toxicities were evaluated.
Results All tumors treated with particle radiotherapy remained controlled without local recurrence at the last follow-up. The overall survival rates for the 16 patients at 1 and 3 years were 61.1 and 36.7%, respectively. We observed a significant difference in the survival rates according to treatment policy. The median survival time was 25.4 months for patients treated with curative intent and 7.7 months for those treated with palliative intent. The one-year survival rates were 100.0 and 33.3%, respectively. No Grade 3 or higher treatment-related toxicities were observed.
Conclusions Particle radiotherapy is thought to be potentially effective and safe for HCC with IVCTT. Considering the current lack of effective and less-invasive local therapy for HCC with IVCTT, particle radiotherapy may therefore be an attractive new therapeutic approach for this type of HCC.

Keywords Hepatocellular carcinoma · Inferior vena cava tumor thrombus · Proton radiotherapy · Carbon ion radiotherapy · Particle radiotherapy

S. Komatsu · T. Fukumoto (✉) · I. Yamada · Y. Hori · Y. Ku
Division of Hepato-Biliary-Pancreatic Surgery,
Department of Surgery, Kobe University Graduate School of Medicine, 7-5-1 Kusunoki-cho, Chuo-ku,
Kobe 650-0017, Japan
e-mail: fukumoto@med.kobe-u.ac.jp

Y. Demizu · K. Terashima · Y. Niwa · M. Mima · O. Fujii · Y. Hishikawa · M. Abe · M. Murakami
Department of Radiology, Hyogo Ion Beam Medical Center,
1-2-1 Kouto, Shingu-cho, Tatsuno, Hyogo 679-5165, Japan

D. Miyawaki · R. Sasaki
Division of Radiation Oncology, Department of Radiology,
Kobe University Graduate School of Medicine,
7-5-1 Kusunoki-cho, Chuo-ku, Kobe 650-0017, Japan

Introduction

Hepatocellular carcinoma (HCC) is one of the most common malignancies worldwide, with the highest incidence being in Asia and Africa [1]. The prognosis of advanced HCC remains poor, particularly in patients with tumor thrombus in the portal vein or the inferior vena cava (IVC). The incidence of portal vein and IVC tumor thrombus (IVCTT) is high in patients with HCC. Autopsy data report these manifestations in as many as 44–84% of HCC patients [2]; clinical data put the figure at 31–50% [3, 4]. Various treatment modalities for HCC have become available and many patients with the disease can be treated effectively [1, 5]. However, the effectiveness of treatments for HCC with an extensive tumor thrombus in the portal vein or IVC is a point of contention.

Advanced HCC with IVCTT has an extremely poor prognosis, with untreated survival reported to be approximately 3 months [6]. Pulmonary tumor embolism

accounted for 6% of deaths from HCC [7]. Intravenous chemotherapy and transarterial chemoembolization (TACE) have yielded only limited improvements in survival [8, 9], and the application of local ablative therapies, such as radiofrequency ablation (RFA), is contraindicated in tumors with vascular invasion [10, 11]. A liver resection is the only effective treatment for HCC with IVCTT, but few patients are suitable candidates due to advanced tumors or coexisting cirrhosis [12]. Patients with advanced HCC with IVCTT need effective local therapy.

Conventional photon radiotherapy for HCC has so far played a limited role in treatment due to the risk of hepatic toxicity that is known as radiation-induced liver disease (RILD) [13, 14]. RILD is still frequent during attempts to deliver a sufficient dose for complete tumor killing, especially for large and/or centrally situated tumors [15]. In contrast, particle beams, such as proton and carbon ion beams, show increased energy deposition and a penetration depth up to a sharp maximum at the end of their range with the aid of the so-called Bragg peak phenomenon. Due to the fact that particle beams minimize doses to the surrounding normal liver, they are suitable for delivering higher doses to liver tumors [16, 17]. Several recent reports have demonstrated the effectiveness of particle radiotherapy for HCC, and it has become widely accepted as a novel treatment option [18–23]. However, the clinical effectiveness of particle radiotherapy for HCC with IVCTT remains uncertain. The aim of this study was to examine the effectiveness and safety of particle radiotherapy for patients who have HCC with IVCTT.

Methods

Patients

The present study was conducted in accordance with the ethical standards set forth by the Declaration of Helsinki, and all patients provided written informed consent. Between June 2001 and January 2009, 349 consecutive patients with HCC were treated with particle radiotherapy at the Hyogo Ion Beam Medical Center. Patients who met the following conditions were ineligible for the treatment: (1) uncontrolled ascites, (2) tumors larger than 15 cm (the upper limit of the irradiation field).

Of the 349 treated patients, 17 had associated tumor thrombi extending into the IVC (Vv3). IVCTT was diagnosed by the identification of an intraluminal filling defect in the IVC shown in contrast-enhanced computed tomography (CT) or magnetic resonance imaging (MRI). One patient discontinued the treatment, with the discontuance not being attributable to irradiation. Therefore, we retrospectively reviewed 16 patients for local tumor control rates, survival rates, and treatment-related toxicities.

The patient and tumor characteristics are summarized in Table 1. All patients were staged according to criteria in the 6th edition of the American Joint Committee on Cancer *AJCC Cancer Staging Manual* [24]. They were divided into 2 groups according to the treatment policy: 6 patients were treated with curative intent (curative treatment group), and the remaining 10 were treated with palliative intent (palliative treatment group). In the curative treatment group, patients had no extrahepatic metastases and all liver tumors detectable on pretreatment imaging could be treated with particle radiotherapy alone ($n = 5$) or in combination with RFA ($n = 1$). All 10 patients in the palliative treatment group had multiple bilobar metastases in the liver that exceeded the limits of RFA. In addition, 8 of these 10 patients had extrahepatic metastases (Stage IV; lung metastases in 6, bone metastasis in 1, lymph node metastases in 2). Palliative treatment was performed to prevent sudden death due to a pulmonary embolism caused by detached tumor thrombi. Regardless of the treatment policy, the main tumors, including the IVCTT, were equally irradiated in both groups. One patient in the curative treatment group and 2 patients in the palliative treatment group had tumors with IVCTT extending into the right atrium. Ten patients (3 in the curative treatment group and 7 in the palliative treatment group) had tumors with portal vein tumor thrombi.

Protocol and treatment planning of particle radiotherapy

Proton beams of 150–210 MeV and carbon ion beams of 250–320 MeV generated by an accelerator with a synchrotron were used for the irradiation. Five protocols for proton radiotherapy, i.e, 56 Gray equivalent (GyE) in 8 fractions; 60 GyE in 10 fractions; 66 GyE in 10 fractions; 76 GyE in 20 fractions; and 76 GyE in 38 fractions were used for treatment, as were two protocols for carbon ion radiotherapy, i.e., 52.8 GyE in 4 fractions and 52.8 GyE in 8 fractions.

Regarding the choice of either the proton or carbon ion beam, the following factors were considered: (1) the percentage of the prescription dose received by at least 95% (D95) of the gross tumor volume (*GTV*); (2) the D95 of the clinical target volume (*CTV*); (3) the D95 of the planning target volume (*PTV*); (4) the percentage of the volume of the noncancerous hepatic portion (entire liver volume minus gross tumor volume) receiving ≥30 GyE (*Liver V30*); (5) the maximum exposure dose of the adjacent gut (Gut Dmax); (6) the percentage of the volume of the adjacent gut receiving ≥40 GyE (Gut V40); (7) the maximum exposure dose of the skin; and (8) the maximum

Table 1 Clinical details of 16 patients treated with particle radiotherapy

Age (years), Sex	PS	Stage group[a]	AFP (ng/ml)	PIVKA II (mAU/ml)	ICG R15 (%)	Child–Pugh grade (score)	Treatment policy	Targeted tumor size (mm)	Protocol GyE/Fr	*Liver V30* (%)	Status, survival time (months)	Hepatic toxicity
83, M	PS0	Stage IIIA	43	1140	3	A (5)	Curative	32 × 28	Proton, 66/10	20	Alive, 17.0	Acute (Grade 2)
61, M	PS0	Stage IIIA	1079	22	16	A (6)	Curative	43 × 43	Proton, 76/38	11	Alive, 26.2	No
70, M	PS1	Stage IIIA	5	139	22	A (5)	Curative	120 × 120	Proton, 76/20	37	Alive, 36.9	Acute (Grade 1), Late (Grade 2)
81, M	PS0	Stage IIIA	304	1060	9	A (5)	Curative	38 × 28	Proton, 60/10	7	Alive, 42.6	Acute (Grade 1)
78, M	PS1	Stage IIIA	38	67	44	A (6)	Curative	30 × 22	Proton, 76/20	9	Dead, 24.3	No
72, F	PS1	Stage IIIA	1612	772	17	A (5)	Curative	36 × 24	Proton, 76/20	17	Dead, 25.6	Acute (Grade 1)
67, M	PS0	Stage IV	37	1810	27	A (5)	Palliative	105 × 105	Proton, 60/10	15	Alive, 8.2	No
45, F	PS0	Stage IV	7	48	8	A (6)	Palliative	130 × 130	Proton, 66/10	36	Alive, 9.9	No
71, M	PS0	Stage IV	1126	69	10	B (8)	Palliative	90 × 90	Carbon, 66/10	31	Alive, 10.5	No
66, F	PS3	Stage IV	62	1420	26	B (7)	Palliative	130 × 130	Carbon, 52.8/8	27	Alive, 13.5	No
66, M	PS0	Stage IV	2270	175000	38	A (6)	Palliative	130 × 130	Proton, 66/10	31	Dead, 3.1	No
52, M	PS0	Stage IIIA	425	6020	18	A (6)	Palliative	48 × 30	Proton, 66/10	24	Dead, 5.5	No
61, M	PS1	Stage IV	6963	5680	17	A (6)	Palliative	110 × 90	Proton, 56/8	15	Dead, 6.0	No
72, F	PS2	Stage IV	660	90000	35	C (10)	Palliative	112 × 56	Proton, 60/10	25	Dead, 6.2	No
55, M	PS2	Stage IV	8	15	16	B (7)	Palliative	100 × 90	Carbon, 52.8/8	28	Dead, 6.7	No
74, M	PS0	Stage IIIA	170	881	21	A (5)	Palliative	32 × 29	Proton, 60/10	13	Dead, 9.9	No

PS performance status, *AFP* alpha-fetoprotein, *PIVKA II* prothrombin induced by vitamin K absence or antagonist II, *ICG R15* indocyanine green retention rate at 15 min, *GyE* gray equivalent radiation dose, *Liver V30* percentage of the volume of the noncancerous hepatic portion (entire liver volume minus gross tumor volume) receiving ≥30 GyE

[a] According to the American Joint Committee on Cancer *Cancer Staging Manual, 6th edition* [24]

exposure dose of the rib. The D95 of the *PTV* and the *Liver V30* have always been high-priority factors, with the *Liver V30* being employed as the most important factor in patients whose liver function has already deteriorated, while the Gut Dmax and/or Gut V40 have become secondary major factors of concern in patients with tumors located close to the gut.

The patients were immobilized with an individually shaped body cast, and beams were synchronized with respiration according to the respiratory gating system. We used a three-dimensional (3D) treatment planning system (FOCUS-M, CMS Japan, Tokyo; and Mitsubishi Electric, Kobe, Japan) with CT–MRI fusion. MRI scans with a 4 mm thickness and consecutive CT images with a 2 mm thickness were obtained for treatment planning. The *CTV* was defined as the *GTV* plus a 5 mm margin. The *PTV* was defined as the 3D isotropic expansion of the *CTV* plus 10 mm. By including 5 mm around the *PTV* as a penumbra, the initial irradiation fields were customized with 3.75 mm width multileaf collimators on the beam's eye view [25]. Portal vein tumor thrombi were also included in the *PTV*.

The doses were calculated on the basis of the pencil beam algorithm. The beam parameters, including the energy level, width of spread-out Bragg peak, and degraded thickness were adequately selected with FOCUS-M. Dose-volume histograms (DVHs) were calculated for all patients to evaluate the irradiated volume and the doses given to the *CTV* and the *PTV*. The particle beam dose is reported in GyE, which is the physical dose multiplied by the relative biological effectiveness of protons or carbon ions. Because all tissues are judged to have approximately the same relative biological effectiveness for protons or carbon ions, the doses expressed in GyE are therefore directly related to photon doses. The *Liver V30* was also evaluated according to the DVH. Based on the findings of several studies of photon radiotherapy, treatment plans at our center are managed to maintain the *Liver V30* at a level within 40% [26, 27]. In patients with Child–Pugh grade B or C, we strictly adhered to this criterion.

Follow-up and evaluation criteria

The patients underwent physical examinations, CT or MRI imaging, and blood tests every 3 months after the treatments. The definition of local recurrence after particle radiotherapy was based on previously established criteria [19, 21, 28]. Local recurrence was defined as the growth of an irradiated tumor or the appearance of new tumors within the *PTV*. Acute and late toxicities associated with treatment were evaluated based on the Radiation Therapy Oncology Group acute radiation morbidity scoring criteria and the Radiation Therapy Oncology Group/European Organization for Research and Treatment of Cancer late radiation morbidity scoring scheme, respectively [29].

Statistical analysis

The Kaplan–Meier method was used for the calculations, and the statistical significance of differences for both local tumor control rates and survival rates was examined using the log-rank test for univariate analysis. *P* values of less than 0.05 were considered to be statistically significant. All statistical analyses were performed with the Statview version 5.0 software package (SAS Institute, Cary, NC, USA).

Results

All patients were followed until their death or until September 2009. Their clinical details are shown in Table 1. Four of the 6 patients in the curative treatment group and 4 of the 10 patients in the palliative treatment group were alive at the last follow-up.

Only one patient (in the curative treatment group, with a single intrahepatic metastasis distant from the primary tumor) underwent proton radiotherapy for the primary tumor and subsequent RFA for the metastatic lesion. The other 15 patients received no other treatments during the particle radiotherapy regimen. Five of the 6 patients in the curative treatment group had new recurrences outside the *PTV* after treatment. Two of them had lung metastases, and the remaining 3 had intrahepatic recurrences. One of the 2 patients with lung metastases received conformal radiation therapy against the lung metastases. All 3 patients with intrahepatic recurrences received treatments in combination with RFA and TACE. The mean period to new recurrence in the curative treatment group after particle radiotherapy was 7.4 months, ranging from 3 to 15 months. None of the 10 patients in the palliative treatment group received any additional treatments after the particle radiotherapy because they selected best supportive care.

Local tumor control rate

Complete local tumor control was achieved in all targeted tumors, including IVCTT. The tumors decreased in size with the passage of time after particle radiotherapy, but did not disappear completely. A representative case presentation, with tumor thrombus extending into the IVC to the right atrium, is shown before and after proton radiotherapy in Fig. 1. The irradiated tumor, including the tumor thrombus, totally disappeared, with recanalization of the IVC and marked shrinkage of the liver parenchyma after treatment.

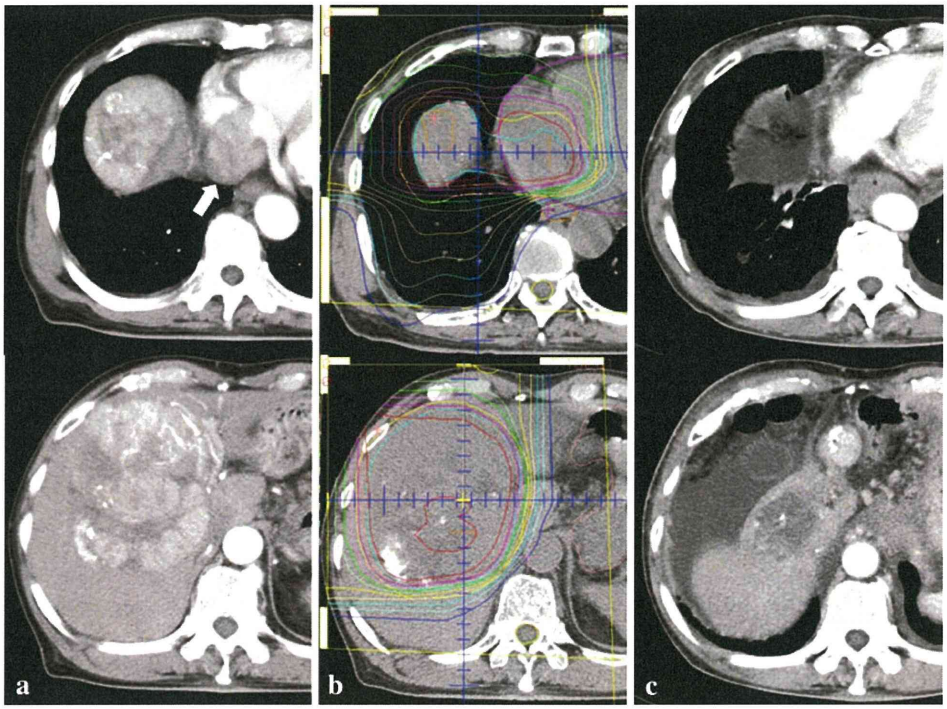

Fig. 1 Findings in a 70-year-old patient demonstrating hepatocellular carcinoma with inferior vena cava tumor thrombus. **a** Contrast-enhanced computed tomography scans before the initiation of proton radiotherapy demonstrated a huge tumor with tumor thrombus extending into the right atrium (*arrow*). **b** Treatment planning of the proton radiotherapy. Isodose curves demonstrate 100% of the prescribed dose at the center and decreasing by 5% of the dose from the inside out. **c** Contrast-enhanced computed tomography scans taken 30 months after completion of proton radiotherapy demonstrated the complete remission of the irradiated tumor including the tumor thrombus, with recanalization of the inferior vena cava and marked shrinkage of the liver parenchyma

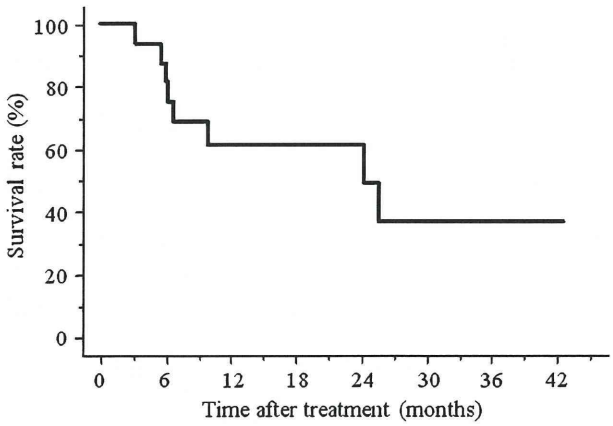

Fig. 2 The overall survival rate of all 16 patients treated with particle radiotherapy is shown

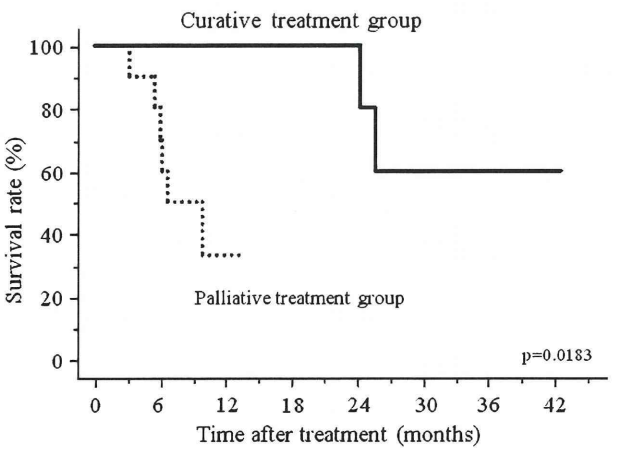

Fig. 3 The overall survival rates according to the treatment policy are shown

Overall survival rates

The overall survival rates for all patients at 1 and 3 years were 61.1 and 36.7%, respectively (Fig. 2). The 1- and 3-year survival rates were 100.0 and 60.0% for patients in the curative treatment group, and 33.3 and 0% for those in the palliative treatment group (Fig. 3). The median survival times in the two groups were 25.4 months and 7.7 months, respectively. A significant difference was observed in overall survival between the two groups ($P = 0.0183$). Five patients in the curative treatment group survived for more than 2 years after treatment, with the longest survival time at 42.6 months. The remaining 1 patient had survived

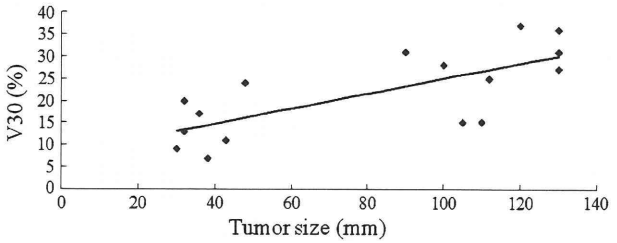

Fig. 4 A scattergram showing the relationship between the tumor size and the *Liver V30* value (percentage of the volume of the noncancerous hepatic portion [entire liver volume minus gross tumor volume] receiving ≥30 gray equivalent radiation dose [GyE])

Table 2 Acute and late toxicities

	Grade 1 No.	Grade 2 No.	Grade 3 No.	Grade 4 No.
Acute toxicities				
Dermatitis	9	2	0	0
Hepatic toxicity	3	1	0	0
Low albuminemia	1	0	0	0
Late toxicities				
Dermatitis	1	0	0	0
Hepatic toxicity	0	1	0	0

for more than 17.0 months after treatment at the last follow-up.

Evaluation of *Liver V30* values

The *Liver V30* values derived from the DVH are shown in Table 1. We plotted the relationship between the tumor size and the *Liver V30* value on a scattergram (Fig. 4). Regardless of tumor size, the *Liver V30* values did not exceed 40%, with an average value of 22% in all cases. The highest *Liver V30* value was 37%, in which the tumor measured 120 mm in greatest dimension. A significant correlation was found between tumor size and *Liver V30* values (the correlation factor was 0.727).

Treatment toxicities

Table 2 shows the treatment-related toxicities in the 16 patients treated with particle radiotherapy. Among the acute toxicities observed, 11 of the 16 patients had dermatitis of grade 2 or less. We observed Grade 2 or less hepatic toxicity in 4 patients, all of whom had no clinically apparent problems. With regard to late toxicities, we observed grade 2 hepatic toxicity in only one patient, whose *Liver V30* value was 37%, the highest among all the patients. However, all acute and late toxicities were transient and tolerable, and they were successfully managed by conservative treatments.

Discussion

This is the first study to demonstrate the efficacy of particle radiotherapy for HCC with IVCTT in a relatively large patient population. The local tumor control rate of HCC with IVCTT was 100.0%, and 1-year survival rates were 61.1% for all patients and 100.0% for patients in the curative treatment group. This result far exceeds any previous data for liver resection, TACE, radiotherapy, and the combination of these modalities for treating HCC with IVCTT [8, 9, 12, 30]; in these studies, the 1-year survival rate of the patients did not exceed 50% with any treatment modality.

To date, liver resection has been the only curative treatment modality for patients who have HCC with IVCTT. Patients for whom liver resection is suitable usually have favorable prognostic factors, such as unifocal lesions, no extrahepatic metastases, and Okuda Stage I [12, 31]. Of the 16 patients in the present study, only 6 patients had these favorable prognostic factors and therefore could be treated with curative intent using particle beams. However, the median survival time of these 6 patients in the present study was 25.4 months, which is much better than that after a liver resection, which has been reported to range from 7 to 8 months [30, 31]. Two possible reasons account for the favorable treatment results of particle radiotherapy in comparison to liver resection for HCC with IVCTT: (1) liver resection for HCC with IVCTT is an invasive procedure that increases the risk of the hematogenous dissemination of tumor cells due to mechanical manipulation during the operation, a factor that accounts for the poor prognosis for a liver resection [32]. In contrast, particle radiotherapy is unrelated to this pattern of tumor development, and (2) surgical stress due to liver resection increases the proliferation of some cytokines, such as vascular endothelial growth factor and hepatocyte growth factor [33, 34], which accelerate tumor growth and invasion [35]. In the absence of surgical stress, particle radiotherapy might minimize the proliferation of these cytokines during and after treatment. Indeed, 4 of the 6 patients in our curative treatment group did not experience extrahepatic metastases after treatment; their median follow-up time was 29.6 months. This result suggests that particle radiotherapy will play a key role in treating HCC with IVCTT. Randomized clinical trials are urgently needed to confirm the best treatment option for these patients.

Historically, the use of external beam radiotherapy for the treatment of HCC has been limited by the poor radiation tolerance of the surrounding liver and subsequent

RILD. Recent improvements of dose localization techniques, including intensity-modulated radiotherapy, conformal 3D planning, and breathing motion management strategies, have made it possible to irradiate smaller, well-defined targets in the liver [36, 37]. However, RILD is still a serious problem in photon radiotherapy. It is especially true with tumors like HCC with IVCTT that are central, deep, and always surrounded by large amounts of normal liver tissues [15]. To compensate for the low antitumor effects of photon beams, a number of radiation fields are needed to deliver a sufficient tumoricidal dose, resulting in increased radiation exposure to the normal liver. Therefore, the application of photon radiotherapy for patients who have HCC with IVCTT has been restricted to small HCCs (<5 cm) or only tumor thrombi [38–41]. Conversely, the highly targeted dose distribution of particle beams exhibited by the Bragg peak enables higher radiation doses to be delivered to tumors, with reduced radiation fields. This significantly lowers the doses to the surrounding normal tissues [16]. Indeed, the *Liver V30* values of all the patients in the present study were less than 40%; nonetheless, most tumors were larger than 5 cm and the tumors, including both the main tumor and the IVCTT were totally irradiated (Fig. 4). In the present study, all treatment-related toxicities developing during or after treatment were transient, easily manageable, and acceptable. The minimal side effects are thought to be associated with the superior dose distribution of the particle beams.

It is obvious that underlying liver disease significantly influences liver damage after radiotherapy. Therefore, treatment targeted to HCC based only on radiation dose-volume analysis should be carefully considered. In this regard, Kawashima et al. [20] proposed that the unirradiated liver volume and pretreatment liver function might be the best indicators for estimating the liver damage after particle radiotherapy. Further studies are required to clarify the upper limit of the radiation dose in combination with liver function in the use of particle radiotherapy to treat HCC.

One of the important clinical questions raised by our data concerns the radiation field of the particle beams in the palliative treatment group. Previous studies of the use of photon radiotherapy on HCC with IVCTT have shown the radiation fields to be focused only on the IVCTT; the main tumors were not included, due to the risk of RILD [38, 39, 41]. However, our data indicate that total irradiation, including the main tumor and the IVCTT, can be safely performed using particle beams. Total irradiation clearly contributed to a longer survival in our curative treatment group in comparison to only a minor survival benefit observed after liver resection. However, the survival benefit of total irradiation in the palliative treatment group remains to be elucidated. The median survival time of the patients in our palliative treatment group was 7.7 months, which was slightly superior to that of untreated patients, which was approximately 3 months [6]. However, it is noteworthy that there were no pulmonary embolic events or sudden deaths after the particle radiotherapy in our study. We hypothesize that the total irradiation may have contributed to reduced growth in the entire tumors, thus leading to a decreased frequency of tumor thrombi dropping into the IVC.

In conclusion, particle radiotherapy appears to be a safe and effective treatment modality for patients who have HCC with IVCTT. Although the number of enrolled patients in the present study was small, our data can serve as a basis for selecting particle radiotherapy as an alternative novel treatment for HCC with IVCTT.

Acknowledgments This study was supported by grants-in-aid for Scientific Research from The Ministry of Education, Culture, Sports, Science and Technology of Japan to Y. Hori (C) (21591773), Y. Ku (C) (20591611), and M. Murakami (B) (22390234), and by grants for the Global Center of Excellence Program for Education and Research on Signal Transduction Medicine in the Coming Generation "Bringing up clinician-scientists in the alliance between basic and clinical medicine" (to Y.K.). The authors declare no conflict of interest.

References

1. Llovet JM, Burroughs A, Bruix J. Hepatocellular carcinoma. Lancet. 2003;362:1907–17.
2. Pirisi M, Avellini C, Fabris C, Scott C, Bardus P, Soardo G, et al. Portal vein thrombosis in hepatocellular carcinoma: age and sex distribution in an autopsy study. J Cancer Res Clin Oncol. 1998;124:397–400.
3. Stuart KE, Anand AJ, Jenkins RL. Hepatocellular carcinoma in the United States. Prognostic features, treatment outcome, and survival. Cancer. 1996;77:2217–22.
4. Fong Y, Sun RL, Jarnagin W, Blumgart LH. An analysis of 412 cases of hepatocellular carcinoma at a Western center. Ann Surg. 1999;229:790–9. (discussion 9–800).
5. Llovet JM, Bruix J. Novel advancements in the management of hepatocellular carcinoma in 2008. J Hepatol. 2008;48(Suppl 1):S20–37.
6. Nagasue N, Yukaya H, Hamada T, Hirose S, Kanashima R, Inokuchi K. The natural history of hepatocellular carcinoma. A study of 100 untreated cases. Cancer. 1984;54:1461–5.
7. Winterbauer RH, Elfenbein IB, Ball WC Jr. Incidence and clinical significance of tumor embolization to the lungs. Am J Med. 1968;45:271–90.
8. Kashima Y, Miyazaki M, Ito H, Kaiho T, Nakagawa K, Ambiru S, et al. Effective hepatic artery chemoembolization for advanced hepatocellular carcinoma with extensive tumour thrombus through the hepatic vein. J Gastroenterol Hepatol. 1999;14:922–7.
9. Chern MC, Chuang VP, Cheng T, Lin ZH, Lin YM. Transcatheter arterial chemoembolization for advanced hepatocellular carcinoma with inferior vena cava and right atrial tumors. Cardiovasc Intervent Radiol. 2008;31:735–44.
10. Lu DS, Raman SS, Limanond P, Aziz D, Economou J, Busuttil R, et al. Influence of large peritumoral vessels on outcome of

radiofrequency ablation of liver tumors. J Vasc Interv Radiol. 2003;14:1267–74.
11. Berber E, Siperstein A. Local recurrence after laparoscopic radiofrequency ablation of liver tumors: an analysis of 1032 tumors. Ann Surg Oncol. 2008;15:2757–64.
12. Fukuda S, Okuda K, Imamura M, Imamura I, Eriguchi N, Aoyagi S. Surgical resection combined with chemotherapy for advanced hepatocellular carcinoma with tumor thrombus: report of 19 cases. Surgery. 2002;131:300–10.
13. Emami B, Lyman J, Brown A, Coia L, Goitein M, Munzenrider JE, et al. Tolerance of normal tissue to therapeutic irradiation. Int J Radiat Oncol Biol Phys. 1991;21:109–22.
14. Lawrence TS, Robertson JM, Anscher MS, Jirtle RL, Ensminger WD, Fajardo LF. Hepatic toxicity resulting from cancer treatment. Int J Radiat Oncol Biol Phys. 1995;31:1237–48.
15. Dawson LA. Protons or photons for hepatocellular carcinoma? Let's move forward together. Int J Radiat Oncol Biol Phys. 2009;74:661–3.
16. Schulz-Ertner D, Tsujii H. Particle radiation therapy using proton and heavier ion beams. J Clin Oncol. 2007;25:953–64.
17. Greco C, Wolden S. Current status of radiotherapy with proton and light ion beams. Cancer. 2007;109:1227–38.
18. Hata M, Tokuuye K, Sugahara S, Kagei K, Igaki H, Hashimoto T, et al. Proton beam therapy for hepatocellular carcinoma with portal vein tumor thrombus. Cancer. 2005;104:794–801.
19. Chiba T, Tokuuye K, Matsuzaki Y, Sugahara S, Chuganji Y, Kagei K, et al. Proton beam therapy for hepatocellular carcinoma: a retrospective review of 162 patients. Clin Cancer Res. 2005;11:3799–805.
20. Kawashima M, Furuse J, Nishio T, Konishi M, Ishii H, Kinoshita T, et al. Phase II study of radiotherapy employing proton beam for hepatocellular carcinoma. J Clin Oncol. 2005;23:1839–46.
21. Bush DA, Hillebrand DJ, Slater JM, Slater JD. High-dose proton beam radiotherapy of hepatocellular carcinoma: preliminary results of a phase II trial. Gastroenterology. 2004;127:S189–93.
22. Nakayama H, Sugahara S, Tokita M, Fukuda K, Mizumoto M, Abei M, et al. Proton beam therapy for hepatocellular carcinoma: the University of Tsukuba experience. Cancer. 2009;115:5499–506.
23. Kato H, Tsujii H, Miyamoto T, Mizoe JE, Kamada T, Tsuji H, et al. Results of the first prospective study of carbon ion radiotherapy for hepatocellular carcinoma with liver cirrhosis. Int J Radiat Oncol Biol Phys. 2004;59:1468–76.
24. Greene FL, Page DL, Fleming ID. AJCC Cancer Staging Manual. 6th ed. New York: Springer; 2002.
25. Mayahara H, Murakami M, Kagawa K, Kawaguchi A, Oda Y, Miyawaki D, et al. Acute morbidity of proton therapy for prostate cancer: the Hyogo Ion Beam Medical Center experience. Int J Radiat Oncol Biol Phys. 2007;69:434–43.
26. Yamada K, Izaki K, Sugimoto K, Mayahara H, Morita Y, Yoden E, et al. Prospective trial of combined transcatheter arterial chemoembolization and three-dimensional conformal radiotherapy for portal vein tumor thrombus in patients with unresectable hepatocellular carcinoma. Int J Radiat Oncol Biol Phys. 2003;57:113–9.
27. Kim TH, Kim DY, Park JW, Kim SH, Choi JI, Kim HB, et al. Dose-volumetric parameters predicting radiation-induced hepatic toxicity in unresectable hepatocellular carcinoma patients treated with three-dimensional conformal radiotherapy. Int J Radiat Oncol Biol Phys. 2007;67:225–31.
28. Mizumoto M, Tokuuye K, Sugahara S, Nakayama H, Fukumitsu N, Ohara K, et al. Proton beam therapy for hepatocellular carcinoma adjacent to the porta hepatis. Int J Radiat Oncol Biol Phys. 2008;71:462–7.
29. Cox JD, Stetz J, Pajak TF. Toxicity criteria of the Radiation Therapy Oncology Group (RTOG) and the European Organization for Research and Treatment of Cancer (EORTC). Int J Radiat Oncol Biol Phys. 1995;31:1341–6.
30. Asahara T, Itamoto T, Katayama K, Nakahara H, Hino H, Yano M, et al. Hepatic resection with tumor thrombectomy for hepatocellular carcinoma with tumor thrombi in the major vasculatures. Hepatogastroenterology. 1999;46:1862–9.
31. Peng SY, Cai XJ, Mu YP, Hong DF, Xu B, Qian HR, et al. Surgical treatment of hepatocellular carcinoma with tumor thrombus in inferior vena cava. Zhonghua Wai Ke Za Zhi. 2006;44:878–81.
32. Liu CL, Fan ST, Cheung ST, Lo CM, Ng IO, Wong J. Anterior approach versus conventional approach right hepatic resection for large hepatocellular carcinoma: a prospective randomized controlled study. Ann Surg. 2006;244:194–203.
33. Kaseb AO, Hanbali A, Cotant M, Hassan MM, Wollner I, Philip PA. Vascular endothelial growth factor in the management of hepatocellular carcinoma: a review of literature. Cancer. 2009;115:4895–906.
34. Chau GY, Lui WY, Chi CW, Chau YP, Li AF, Kao HL, et al. Significance of serum hepatocyte growth factor levels in patients with hepatocellular carcinoma undergoing hepatic resection. Eur J Surg Oncol. 2008;34:333–8.
35. Qin LX, Tang ZY. The prognostic molecular markers in hepatocellular carcinoma. World J Gastroenterol. 2002;8:385–92.
36. Tse RV, Guha C, Dawson LA. Conformal radiotherapy for hepatocellular carcinoma. Crit Rev Oncol Hematol. 2008;67:113–23.
37. Cheng JC, Wu JK, Huang CM, Liu HS, Huang DY, Tsai SY, et al. Dosimetric analysis and comparison of three-dimensional conformal radiotherapy and intensity-modulated radiation therapy for patients with hepatocellular carcinoma and radiation-induced liver disease. Int J Radiat Oncol Biol Phys. 2003;56:229–34.
38. Zeng ZC, Fan J, Tang ZY, Zhou J, Qin LX, Wang JH, et al. A comparison of treatment combinations with and without radiotherapy for hepatocellular carcinoma with portal vein and/or inferior vena cava tumor thrombus. Int J Radiat Oncol Biol Phys. 2005;61:432–43.
39. Zeng ZC, Fan J, Tang ZY, Zhou J, Wang JH, Wang BL, et al. Prognostic factors for patients with hepatocellular carcinoma with macroscopic portal vein or inferior vena cava tumor thrombi receiving external-beam radiation therapy. Cancer Sci. 2008;99:2510–7.
40. Hawkins MA, Dawson LA. Radiation therapy for hepatocellular carcinoma: from palliation to cure. Cancer. 2006;106:1653–63.
41. Koo JE, Kim JH, Lim YS, Park SJ, Won HJ, Sung KB, et al. Combination of transarterial chemoembolization and three-dimensional conformal radiotherapy for hepatocellular carcinoma with inferior vena cava tumor thrombus. Int J Radiat Oncol Biol Phys. 2009;78(1):180–7.

Original Article

Clinical Results and Risk Factors of Proton and Carbon Ion Therapy for Hepatocellular Carcinoma

Shohei Komatsu, MD[1,2]; Takumi Fukumoto, MD, PhD[1]; Yusuke Demizu, MD, PhD[2]; Daisuke Miyawaki, MD, PhD[3]; Kazuki Terashima, MD[2]; Ryohei Sasaki, MD, PhD[3]; Yuichi Hori, MD, PhD[1]; Yoshio Hishikawa, MD, PhD[2]; Yonson Ku, MD, PhD[1]; and Masao Murakami, MD, PhD[2]

BACKGROUND: The objective of this study was to evaluate the clinical outcome of proton and carbon ion therapy for hepatocellular carcinoma (HCC). **METHODS:** In total, 343 consecutive patients with 386 tumors, including 242 patients (with 278 tumors) who received proton therapy and 101 patients (with 108 tumors) who received carbon ion therapy, were treated on 8 different protocols of proton therapy (52.8-84.0 gray equivalents [GyE] in 4-38 fractions) and on 4 different protocols of carbon ion therapy (52.8-76.0 GyE in 4-20 fractions). **RESULTS:** The 5-year local control and overall survival rates for all patients were 90.8% and 38.2%, respectively. Regarding proton and carbon ion therapy, the 5-year local control rates were 90.2% and 93%, respectively, and the 5-year overall survival rates were 38% and 36.3%, respectively. These rates did not differ significantly between the 2 therapies. Univariate analysis identified tumor size as an independent risk factor for local recurrence in proton therapy, carbon ion therapy, and in all patients. Multivariate analysis identified tumor size as the only independent risk factor for local recurrence in proton therapy and in all patients. Child-Pugh classification was the only independent risk factor for overall survival in proton therapy, in carbon ion therapy, and in all patients according to both univariate and multivariate analyses. No patients died of treatment-related toxicities. **CONCLUSIONS:** Proton and carbon ion therapies for HCC were comparable in terms of local control and overall survival rates. These therapies may represent innovative alternatives to conventional local therapies for HCC. ***Cancer* 2011;117:4890–904.** © *2011 American Cancer Society.*

KEYWORDS: hepatocellular carcinoma, particle therapy, proton therapy, carbon ion therapy, local recurrence.

Hepatocellular carcinoma (HCC) is the fifth leading cause of cancer death worldwide, and the majority of patients with HCC reside in Asian countries.[1,2] HCC is well suited to local therapy, because it has a tendency to stay within the liver, and distant metastasis generally occurs late. This implies that curative local therapy, as represented by hepatectomy and liver transplantation, has a great impact on the disease course and also offers the best chance of long-term survival for patients with HCC.[3,4] However, only 5% to 40% of patients with HCC are amenable to a hepatectomy because of either advanced tumors or coexisting cirrhosis,[5,6] and a shortage of liver grafts limits the applicability of liver transplantation. Although local ablative therapies, such as radiofrequency ablation (RFA), recently have gained widespread clinical acceptance, there is growing evidence of a high local recurrence rate after RFA that reaches up to 36%.[7,8] In addition, local ablative therapies also are unsuitable for patients who have bleeding tendencies, unfavorable anatomic tumor locations, or large tumors.[8,9] Patients who are not eligible for local ablative therapies usually receive noncurative modalities, such as transarterial chemoembolization (TACE) or systemic chemotherapy.

Radiotherapy also is a local therapy but historically has played a limited role in the treatment of HCC, because the hepatic tolerance dose is lower than the tumoricidal dose, especially when liver function is impaired by chronic liver disease.[10-12] Particle beams, such as proton and carbon ion beams, have demonstrated an increase in energy deposition with a penetration depth up to a sharp maximum at the end of their range: the so-called Bragg peak phenomenon.[13] Therefore, higher tumor doses can be delivered without increasing toxicity to the surrounding noncancerous tissues and organs. Particle therapy results for HCC have been reported in several case series, all of which have reported good overall survival and encouraging local control rates.[14-19] However, most of those studies were conducted at proton treatment centers, and few

Corresponding author: Takumi Fukumoto, MD, PhD, Department of Surgery, Division of Hepato-Biliary-Pancreatic Surgery, Kobe University Graduate School of Medicine, 7-5-1 Kusunoki-cho, Chuo-ku, Kobe 650-0017, Japan; Fax: (011) 81-78-382-6307; fukumoto@med.kobe-u.ac.jp

[1]Department of Surgery, Division of Hepato-Biliary-Pancreatic Surgery, Kobe University Graduate School of Medicine, Kobe, Japan; [2]Department of Radiology, Hyogo Ion Beam Medical Center, Tatsuno, Japan; [3]Department of Radiology, Division of Radiation Oncology, Kobe University Graduate School of Medicine, Kobe, Japan

DOI: 10.1002/cncr.26134, **Received:** December 12, 2010; **Revised:** February 20, 2011; **Accepted:** February 23, 2011, **Published online** April 14, 2011 in Wiley Online Library (wileyonlinelibrary.com)

Table 1. Patient Characteristics

Characteristic	No. of Patients (%)		
	Proton Therapy, n=242	Carbon Ion Therapy, n=101	All Patients, n=343
Age, y			
<70	115 (48)	55 (54)	170 (50)
≥70	127 (52)	46 (46)	173 (50)
Sex			
Men	182 (75)	73 (72)	255 (74)
Women	60 (25)	28 (28)	88 (26)
Positive viral marker			
Hepatitis B virus	27 (11)	19 (19)	46 (13)
Hepatitis C virus	159 (66)	60 (59)	219 (64)
None	54 (22)	21 (21)	75 (22)
Both	2 (1)	1 (1)	3 (1)
Performance status			
0	172 (71)	73 (72)	245 (71)
1	57 (24)	18 (18)	75 (22)
2	10 (4)	9 (9)	19 (6)
3	3 (1)	1 (1)	4 (1)
Child-Pugh classification			
A	184 (76)	78 (77)	262 (76)
B	55 (23)	20 (20)	75 (22)
C	3 (1)	3 (3)	6 (2)
BCLC stage			
0	9 (4)	9 (9)	18 (5)
A	82 (34)	36 (36)	118 (34)
B	32 (13)	15 (15)	47 (14)
C	113 (47)	37 (36)	150 (44)
D	6 (2)	4 (4)	10 (3)
Recommended treatment according to BCLC stage			
Resection: Operable group	49 (20)	29 (29)	78 (23)
Others: Inoperable group	193 (80)	72 (71)	265 (77)
No. of tumors			
Single	213 (88)	81 (80)	294 (86)
Multiple	29 (12)	20 (20)	49 (14)

Abbreviations: BCLC, Barcelona Clinic Liver Cancer.

studies have reported results of carbon ion therapy for HCC. To our knowledge, no reports have focused on the differences in treatment results between the 2 types of particle beams.

The Hyogo Ion Beam Medical Center (HIBMC) is the only facility in the world that provides both proton and carbon ion therapies.[20] In the current study, we analyzed the efficacy and safety of proton and carbon ion therapy for HCC at the HIBMC.

MATERIALS AND METHODS

Patient and Tumor Characteristics

The current study was conducted according to the Helsinki Declaration, and written informed consent was obtained from all patients. From May 2001 to January 2009, 343 consecutive patients with 400 HCCs were treated at the HIBMC (excluding 6 patients who discontinued treatment). Patients who met the following conditions were ineligible for treatment: 1) uncontrolled ascites and 2) tumors that measured >15 cm in greatest dimension (the upper limit of the irradiation field). No patients were lost to follow-up, although we could not evaluate the post-treatment imaging findings from 12 patients with 14 tumors. Thus, overall survival rates were determined for all 343 patients, and local control rates were determined for 386 tumors. In total, 242 patients with 278 tumors received proton therapy, and 101 patients with 108 tumors received carbon ion therapy. For all patients,

Table 2. Tumor Characteristics

Characteristic	No. of Tumors (%)		
	Proton Therapy, n=278	Carbon Ion Therapy, n=108	All Patients, n=386
Tumor size, mm			
<50	196 (71)	81 (75)	277 (72)
50-100	65 (23)	22 (20)	87 (22)
>100	17 (6)	5 (5)	22 (6)
Gross classification			
Single nodular type	153 (55)	54 (50)	207 (53)
Single nodular with extranodular growth type	85 (30)	41 (38)	126 (33)
Confluent multinodular type	13 (5)	6 (6)	19 (5)
Infiltrative type	27 (10)	7 (6)	34 (9)
Macroscopic vascular invasion			
Yes	73 (26)	19 (18)	92 (24)
No	205 (74)	89 (82)	294 (76)
Perivascular location			
Yes	121 (44)	32 (30)	153 (40)
No	157 (56)	76 (70)	233 (60)
Prior treatment history to the target tumor			
Yes	132 (47)	49 (45)	181 (47)
No	146 (53)	59 (55)	205 (53)
Serum AFP, ng/mL			
<100	184 (66)	72 (67)	256 (66)
≥100	94 (34)	36 (33)	130 (34)
Serum PIVKAII, mAU/mL			
<100	129 (46)	58 (54)	187 (48)
≥100	149 (54)	50 (46)	199 (52)

Abbreviations: AFP, α-fetoprotein; PIVKAII, protein induced by vitamin K absence or antagonist II.

HCC was diagnosed on the basis of the results from imaging studies, which usually included a combination of contrast-enhanced computed tomography (CT) and magnetic resonance imaging (MRI) studies. Tumor markers, including serum α-fetoprotein (AFP) and serum protein induced by vitamin K absence or antagonist II (PIVKAII), also were measured before and after treatment. Chest CT scans, bone scintigrams, and positron-emission tomography studies, if necessary, were obtained to exclude the possibility of distant metastasis.

Patient and tumor characteristics are summarized in Tables 1 and 2, respectively, for the proton and carbon ion therapy groups and for all patients. All the patients were staged and categorized as either operable (operable group) or inoperable (inoperable group) according to Barcelona Clinic Liver Cancer (BCLC) classification criteria.[21] Tumors were classified into 3 groups according to tumor size (<50 mm, 50-100 mm, and >100 mm). All tumors were divided grossly into 4 types according to Liver Cancer Study Group of Japan criteria[22]: 1) single nodular type, 2) single nodular type with extranodular growth, 3) confluent multinodular type, and 4) infiltrative type. Studies have indicated that single nodular type tumors have a better prognosis than the other tumor types;[23] therefore, all tumors were categorized further as either single nodular type or nonsingle nodular type. Macroscopic vascular invasion was defined as gross tumor vascular invasion into the portal or hepatic veins identified by pretreatment imaging. Perivascular location was defined as a situation in which the tumor invaded or abutted the main portal trunk and/or inferior vena cava. Among the 181 tumors that had received treatment before particle therapy, 2 tumors were classified as local recurrences after hepatectomy, and 60 tumors were classified as local recurrences after percutaneous local therapy. In addition, 169 target tumors had undergone TACE before particle therapy. All data were analyzed retrospectively for proton and carbon ion therapy, and all patients were considered with regard to local tumor control rates, overall patient survival rates, and treatment-related toxicities.

Table 3. Treatment Protocols

BED_{10}[a]	Protocol (BED_{10})	No. of Patients [%]
Proton therapy		
<100	76 GyE/38 Fr (91.2)	11 [4]
	56 GyE/8 Fr (95.2)	4 [2]
	60 GyE/10 Fr (96.0)	89 [37]
≥100	76 GyE/20 Fr (104.88)	70 [29]
	66 GyE/10 Fr (109.56)	53 [22]
	80 GyE/20 Fr (112)	3 [1]
	84 GyE/20 Fr (119.28)	3 [1]
	52.8 GyE/4 Fr (122.496)	9 [4]
Carbon ion therapy		
<100	52.8 GyE/8 Fr (87.648)	23 [23]
≥100	76 GyE/20 Fr (104.88)	3 [3]
	66 GyE/10 Fr (109.56)	16 [16]
	52.8 GyE/4 Fr (122.496)	59 [58]

Abbreviations: BED_{10}, biologic effective dose for acute-reacting tissues; Fr, fractions; GyE, gray equivalents.
[a] The BED_{10} was calculated by linear-quadratic formalism assuming an α/β ratio of 10 GyE.

Treatment Protocol

The biologic effects of both proton and carbon ion therapy at the HIBMC were evaluated in vitro and in vivo, and the relative biologic effectiveness (RBE) values of these therapies were determined as 1.1 and 2,0 to 3.7, respectively (depending on the depth of the spread-out Bragg peaks).[24] Because we assumed that all tissues had almost the same RBE for protons or carbon ions, doses expressed in gray equivalents (GyE), were directly comparable to photon doses.

Eight protocols for proton therapy (52.8-84 GyE in 4-38 fractions using 150-megaelectron volt [MeV], 190-MeV, 210-MeV, or 230-MeV proton beams) and 4 protocols for carbon ion therapy (52.8-76 GyE in 4-20 fractions using 250-MeV or 320-MeV carbon ion beams) were used during the study period (Table 3). The radiobiologic equivalent dose for acute-reacting tissues (BED_{10}) was calculated for each protocol. The protocols for proton and carbon ion therapy were set first on the basis of earlier experience at the National Cancer Center East (Kashiwa, Japan), the Proton Medical Research Center (Tsukuba, Japan), and the National Institute of Radiological Sciences (Chiba, Japan). Thereafter, we adopted dose-escalation or hypofractionation protocols, depending on patient and tumor factors.

The policy for the selection of beam type was determined by the following: 1) from May to October 2001 and from April 2003 to March 2005, only proton therapy was available (52 patients with 57 tumors); 2) from February to June 2002, only carbon ion therapy was available (6 patients with 6 tumors); and 3) since April 2005, treatment plans for both proton and carbon ion therapy were made for all patients, and a better suited beam was selected on the basis of the treatment plans (285 patients with 323 tumors). Regarding the choice of either proton beam or carbon ion beam therapy, the following factors were considered: 1) the values for the percentage prescription dose received by at least 95% volume (D95) of the gross tumor volume (GTV), 2) D95 of the clinical target volume (CTV), 3) D95 of the planning target volume (PTV), 4) the percentage of the volumes of hepatic noncancerous portions (entire liver volume − GTV) receiving ≥30 GyE (Liver V30), 5) the maximum exposure doses of the adjacent gut (Gut Dmax), 6) the percentage of the volumes of the adjacent gut receiving ≥40 GyE (Gut V40), 7) the maximum exposure doses to the skin, and 8) the maximum exposure doses to the ribs. D95 of the PTV and Liver V30 values have always been high-priority factors. Among these factors, Liver V30 is used as the most important factor for patients whose liver function already has deteriorated, and Gut Dmax and/or Gut V40 values have become secondary major concerning factors in patients who have tumors located close to the gut.

A representative case presentation of treatment plans for both proton therapy and carbon ion therapy is provided in Figure 1. The D95 of PTV was equal for proton and carbon ion therapy. Conversely, Gut Dmax and Gut V40 were significantly higher for the proton treatment plan than for the carbon ion treatment plan. Therefore, carbon ion therapy was selected in this representative case.

Treatment Planning

The radiation treatments were designed to use a CT-based, 3-dimensional treatment planning system (FOCUS-M; CMS, Tokyo, Japan; and Mitsubishi Electric, Kobe, Japan). CT images were obtained at the phase of expiration using a respiratory gating system. A respiratory gating irradiation system that was developed at the National Institute of Radiological Sciences in Chiba[25] was used for irradiation of the beam during the exhalation phase for all patients. The GTV and the organs at a risk of irradiation, such as the liver and intestines, were delineated according to fusion images that were constructed from contrast-enhanced CT and MRI studies. Treatment planning was defined as follows: CTV = GTV + 5 mm, PTV = CTV + 5 mm. In addition, another 5-mm to 10-mm margin was included in the caudal axis to compensate for uncertainty caused by respiration-induced